**Supplementary Information for**

# Synthesis and Reactivity of Cobalt-Dinitrogen Complexes Bearing Anionic PCP-type Pincer Ligands toward Catalytic Silylamine Formation from Dinitrogen

Shogo Kuriyama,† Shenglan Wei,† Hiromasa Tanaka,‡ Asuka Konomi,§ Kazunari Yoshizawa,§* and Yoshiaki Nishibayashi†*

†Department of Applied Chemistry, School of Engineering, The University of Tokyo, Hongo, Bunkyo-ku, Tokyo 113-8656, Japan.

‡School of Liberal Arts and Sciences, Daido University, Minami-ku, Nagoya 457-8530

§Institute for Materials Chemistry and Engineering, Kyushu University, Nishi-ku, Fukuoka 819-0395

**Contents**

**General Methods.**

$^{1}H$ NMR (400 MHz), $^{13}C\{^{1}H\}$ NMR (100 MHz), $^{31}P\{^{1}H\}$ NMR (162 MHz), and $^{19}F$ NMR (376 Hz) spectra were recorded on a JEOL ECS-400 spectrometer or a JEOL ECZ-400S spectrometer in suitable solvent, and spectra were referenced to residual solvent ($^{1}H$, $^{13}C\{^{1}H\}$) or external standard ($^{31}P\{^{1}H\}$: $H_3PO_4$; $^{19}F$: $CF_3C_6H_5$). IR spectra were recorded on a JASCO FT/IR 4100 Fourier Transform infrared spectrometer or a Shimadzu IRSpirit spectrometer. UV-vis absorption spectra were recorded on a Shimadzu UV-1850. Gas chromatography (GC) analyses for the quantification of $N(SiMe_3)_3$ and byproducts were carried out on a Shimadzu GC-2014 instrument equipped with a flame-ionization detector using CBP 10 fused silica capillary column (25 m × 0.25 mm). Gas chromatography−mass spectroscopy (GC−MS) was performed on a Shimadzu GCMS-QP2010 PLUS instrument. Mass spectra were measured on a JEOL JMS-700 mass spectrometer. Magnetic susceptibility was measured in $C_6D_6$ using the Evans method.[S1] Elemental analyses were performed at Microanalytical Center of The University of Tokyo.

All manipulations were carried out under an atmosphere of nitrogen or argon by using standard Schlenk techniques or glovebox techniques unless otherwise stated. Solvents were dried by general methods and degassed before use. $Me_3SiCl$ was distilled prior to use. 2-Bromo-1,3-bis(dibromomethyl)-5-methoxybenzene,[S2] 2-bromo-1,3-bis(bromomethyl)-5-*tert*-butylbenzne,[S3] 4-(3,5-bis(trifluoromethyl)phenyl)-2,6-dimethylbromobenzene,[S4] di-*tert*-butylphosphine,[S5] and $KC_8$[S6] were prepared according to the literature methods. All the other reagents were commercially available.

**Preparation of Ligands and Cobalt Complexes.**

Preparation of 2-bromo-1,3-bis(bromomethyl)-5-(3,5-bis(trifluoromethyl)phenyl)benzene (**4**).

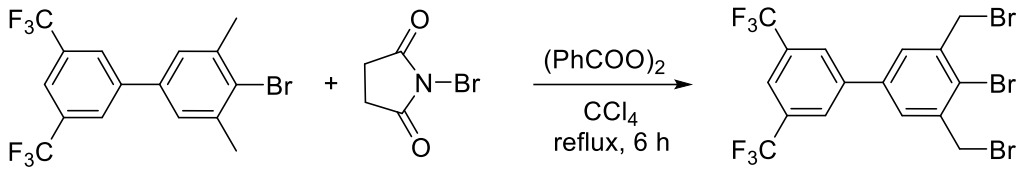


**4**

A mixture of 4-(3,5-bis(trifluoromethyl)phenyl)-2,6-dimethylbromobenzene (596 mg, 1.50 mmol), N-bromosuccinimide (643 mg, 3.61 mmol), and benzoyl peroxide (15.0 mg, 0.062 mmol) in $CCl_4$ (20 mL) was stirred at reflux temperature for 3 h. After solvent was removed *in vacuo*, the residue was purified by $SiO_2$ column chromatography (hexane) to afford **4** as a white solid (758 mg, 1.37 mmol, 91%). $^1$H NMR ($CDCl_3$): δ 7.99 (s, 2H), 7.92 (s, 1H), 7.63 (s, 2H), 4.72 (s, 4H). $^{13}$C{$^1$H} NMR ($CDCl_3$): δ 141.1, 139.9, 138.4, 132.4 (q, $J$ = 33.6 Hz), 130.9, 129.9, 127.3 (d, $J$ = 13.4 Hz), 123.3 (q, $J$ = 269.0 Hz), 122.0–121.9 (m), 33.4. $^{19}$F NMR ($CDCl_3$): δ -62.7 (s). HRMS(FAB) Calcd. for $C_{16}H_9Br_3P_6$ $[M+H]^+$: 553.8140. Found 553.8139.

Preparation of $^R$PCP–Br.

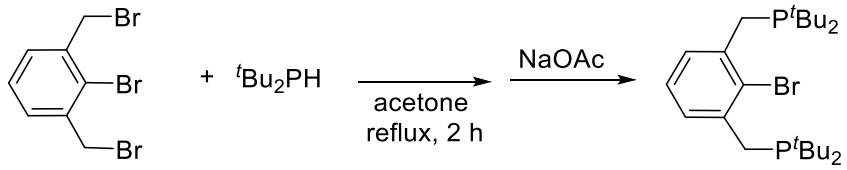


$^H$PCP-Br

A typical experimental procedure for the synthesis of $^H$PCP–Br is described below. A mixture of 2-bromo-1,3-bis(bromomethyl)benzene (2.61 g, 7.61 mmol) and $^t$Bu$_2$PH (2.94 g, 20.1 mmol) in acetone (55 mL) was stirred at reflux temperature for 2 h. After cooling to room temperature, the solvent was removed *in vacuo*, then the residue was washed with $Et_2O$ (8 mL, 3 times). After the addition of NaOAc (5.0 g), $Et_2O$ (20 mL), and water (15 mL) to the white residue, the product was extracted by $Et_2O$ (15 mL, 3 times). After the combined extracts were dried over anhydrous $MgSO_4$, the mixture was filtered, and the filtrate was evaporated to dryness to afford PCP-Br as a white solid (2.83 g, 5.98 mmol, 79%). $^1$H NMR ($C_6D_6$): δ 7.68 (d, $J$ = 7.6 Hz, 2H), 7.04 (t, $J$ = 7.6 Hz, 1H), 3.11 (s, 4H), 1.10 (d, $J$ = 10.8 Hz, 36H). $^{13}$C{$^1$H} NMR ($C_6D_6$): δ 141.9 (d, $J$ = 13.4 Hz), 130.0 (d, $J$ = 19.1 Hz), 128.5, 126.5, 32.0 (d, $J$ = 23.9 Hz), 29.8 (d, $J$ = 14.3

Hz), 29.7 (d, $J$ = 24.8 Hz). $^{31}P\{^{1}H\}$ NMR ($C_6D_6$): δ 34.1 (s). Anal. Calcd. for $C_{24}H_{43}BrP_2$: C, 60.88; H, 9.15. Found: C, 60.87, H, 9.03.

Isolated yields and analytical data of $^{MeO}$PCP–Br, $^{t\text{Bu}}$PCP–Br and $^{ArF}$PCP–Br are summarized below.

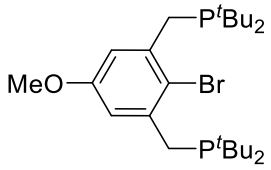


$^{MeO}$PCP-Br

$^{MeO}$PCP–Br: 80% yield. A white solid. $^{1}H$ NMR ($C_6D_6$): δ 7.51 (d, $J$ = 2.4 Hz, 2H), 3.42 (s, 3H), 3.14 (d, $J$ = 2.8 Hz, 4H), 1.11 (d, $J$ = 10.8 Hz, 36H). $^{13}C\{^{1}H\}$ NMR ($C_6D_6$): δ 158.5, 142.8 (d, $J$ = 13.4 Hz), 119.3, 115.9 (d, $J$ = 20.1 Hz), 54.8, 32.0 (d, $J$ = 23.9 Hz), 29.8 (d, $J$ = 13.4 Hz), 29.7 (d, $J$ = 24.0 Hz). $^{31}P\{^{1}H\}$ NMR ($C_6D_6$): δ 34.0 (s). Anal. Calcd. for $C_{25}H_{45}BrOP_2$: C, 59.64; H, 9.01. Found: C, 59.33, H, 8.84.

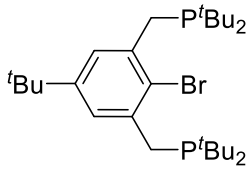


$^{t\text{Bu}}$PCP-Br

$^{t\text{Bu}}$PCP–Br: 89% yield. A colorless oil. $^{1}H$ NMR ($C_6D_6$): δ 7.89 (s, 2H), 3.18 (d, $J$ = 2.8 Hz, 4H), 1.35 (s, 9H), 1.13 (d, $J$ = 10.4 Hz, 36H). $^{13}C\{^{1}H\}$ NMR ($C_6D_6$): δ 149.0, 141.0 (d, $J$ = 11.5 Hz), 127.5 (d, $J$ = 21.1 Hz), 125.6, 34.7, 32.0 (d, $J$ = 24.0 Hz), 31.3, 29.9 (d, $J$ = 13.4 Hz), 29.9 (d, $J$ = 26.8 Hz). $^{31}P\{^{1}H\}$ NMR ($C_6D_6$): δ 33.3 (s). HRMS(FAB) Calcd. for $C_{28}H_{51}BrP_2$ $[M+H]^+$: 529.2728. Found 529.2711.

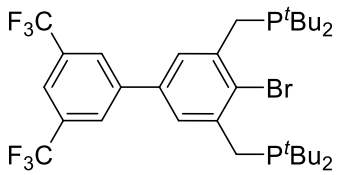


$^{ArF}$PCP-Br

Ar$^F$-PCP-Br (Ar$^F$ = 3,5-bis(trifluoromethyl)phenyl): 89% yield. A white solid. $^{1}H$ NMR ($C_6D_6$): δ 7.95–7.94 (m, 4H), 7.64 (s, 1H), 3.18 (d, $J$ = 2.4 Hz, 4H), 1.10 (d, $J$ = 11.2 Hz, 36H). $^{13}C\{^{1}H\}$ NMR ($C_6D_6$): δ 143.3 (d, $J$ = 12.4 Hz), 143.1, 136.4, 132.4 (q, $J$ =

32.9 Hz), 129.4, 128.7 (d, $J$ = 19.2Hz), 127.2, 123.8 (q, $J$ = 271.2 Hz), 121.2, 32.1 (d, $J$ = 24.0 Hz), 29.8 (d, $J$ = 13.4 Hz), 29.7 (d, $J$ = 26.8 Hz). $^{31}P\{^{1}H\}$ NMR ($C_6D_6$): δ 36.1 (s). $^{19}F$ ($C_6D_6$): δ -62.5 (s). HRMS(FAB) Calcd. for $C_{32}H_{45}BrF_6P_2$ $[M+H]^+$: 684.2084. Found 684.2050.

Preparation of **2a**–**2d**.

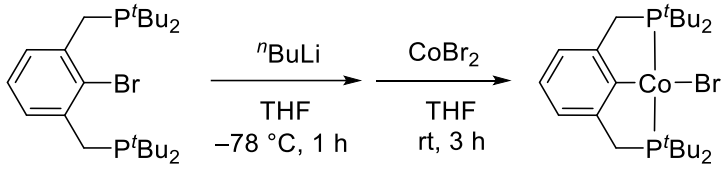


$^H$PCP-Br **2a**

A typical experimental procedure for the synthesis of **2a** is described below. A solution of $^H$PCP-Br (237 mg, 0.501 mmol) in THF (5 mL) was added $^n$BuLi (1.55 M in hexane, 325 μL, 0.504 mmol) at –78 ºC. After the mixture was stirred at –78 ºC for 1 h, a suspension of $CoBr_2$ (109 mg, 0.498 mmol) in THF (5 mL) was added to the mixture. After the reaction mixture was stirred at room temperature for 4 h, the solvent was removed *in vacuo*. After the addition of hexane (10 mL) to the brown residue, the suspension was filtered through Celite, and the filter cake was washed with hexane (3 mL, 4 times). The combined filtrate was dried *in vacuo*. The obtained yellow solid was washed with a small amount of cold pentane and dried *in vacuo* to afford **2a** as a yellow solid (227 mg, 0.426 mmol, 86%). Single crystals of **2a** suitable for X-ray crystallography were obtained as yellow crystals from hexane at –30 ºC. $^1H$ NMR ($C_6D_6$): δ 52.3, 11.2, –20.5, –20.9. Magnetic susceptibility (Evans' Method): $\mu_{eff}$ = 2.4(1) $\mu$B in $C_6D_6$ at 298 K. Anal. Calcd. for $C_{24}H_{43}BrP_2Co$: C, 54.14; H, 8.14. Found: C, 54.08; H, 7.94.

Isolated yields and analytical data of **2b**, **2c** and **2d** are summarized below.

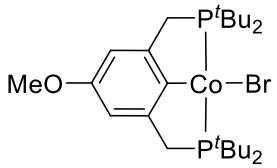


**2b**

**2b**: 64% yield. Yellow crystals. Single crystals of **2b** suitable for X-ray crystallography were obtained as yellow crystals from hexane at –30 ºC. $^1H$ NMR ($C_6D_6$): δ 65.1, 12.4, –0.6, –15.9. Magnetic susceptibility (Evans' Method): $\mu_{eff}$ = 2.5(1) $\mu$B in $C_6D_6$ at 298

K. Anal. Calcd. for $C_{25}H_{45}BrOP_2Co$: C, 53.39; H, 8.07. Found: C, 53.48; H, 7.68.

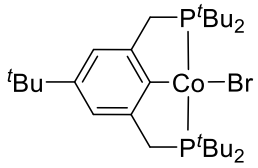


**2c**

**2c**: 51% yield. Yellow crystals. $^1$H NMR ($C_6D_6$): δ 11.8, –4.4, –19.4. Magnetic susceptibility (Evans' Method): $\mu_{eff}$ = 2.4(1) $\mu$B in $C_6D_6$ at 298 K. Anal. Calcd. for $C_{28}H_{51}BrP_2Co$: C, 57.15; H, 8.74. Found: C, 57.38; H, 8.51.

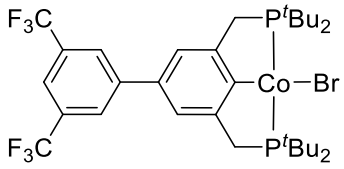


**2d**

**2d**: 50% yield. Yellow crystals. Single crystals of **2d** suitable for X-ray crystallography were obtained as yellow crystals from hexane at –30 ºC. $^1$H NMR ($C_6D_6$): δ 44.5, 10.1, 5.1, 2.7, –18.8. Magnetic susceptibility (Evans' Method): $\mu_{eff}$ = 2.3(1) $\mu$B in $C_6D_6$ at 298 K. Anal. Calcd. for $C_{32}H_{45}BrF_6P_2Co$: C, 51.63; H, 6.09. Found: C, 51.57; H, 5.75.

Preparation of **3a**–**3d**.

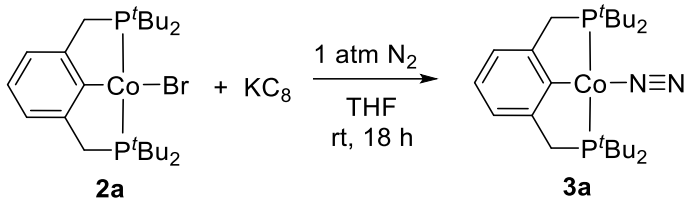


**2a** **3a**

A typical experimental procedure for the synthesis of **3a** is described below. To a 20 mL Schlenk flask containing **2a** (104 mg, 0.195 mmol) and $KC_8$ (28.9 mg, 0.214 mmol) was added THF (4 mL) under $N_2$ (1 atm). After stirring at room temperature for 18 h under $N_2$ (1 atm), the solvent was removed *in vacuo*. After the addition of hexane (5 mL) to the purple residue, the suspension was filtered through Celite, and the filter cake was washed with hexane (2 mL, 4 times). The combined filtrate was dried *in vacuo*. The obtained purple solid was washed with a small amount of cold pentane and dried *in vacuo* to afford **3a** as a purple solid (67.6 mg, 0.141 mmol, 72%). Single crystals of **3a** suitable for X-ray crystallography were obtained as purple crystals from hexane at –30 ºC. $^1$H NMR ($C_6D_6$): δ 7.01 (s, 3H), 3.21 (t, $J$ = 3.4 Hz, 4H), 1.35 (t, $J$ = 6.2 Hz, 36H). $^{31}$P{$^1$H} NMR ($C_6D_6$): δ 91.6 (br s). IR (KBr, $\nu_{NN}$) 2007 cm$^{-1}$, IR (THF, $\nu_{NN}$) 2009 cm$^{-1}$, IR (neat, ATR, $\nu_{NN}$) 2002 cm$^{-1}$. Anal. Calcd. for $C_{24}H_{43}N_2P_2Co$: C, 59.99; H, 9.02; N, 5.83. Found: C, 59.84; H, 9.05; N, 5.02. The slightly low content of nitrogen is considered to be due to the labile property of the coordinated dinitrogen in **3a**.

Isolated yields and analytical data of **3b**, **3c** and **3d** are summarized below.

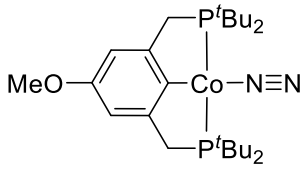


**3b**

**3b**: 45% yield. Purple crystals. Single crystals of **3b** suitable for X-ray crystallography were obtained as purple crystals from hexane at –30 ºC. $^1$H NMR ($C_6D_6$): δ 6.70 (s, 2H), 3.51 (s, 3H), 3.16 (t, $J$ = 3.2 Hz, 4H), 1.37 (t, $J$ = 6.0 Hz, 36H). $^{31}$P{$^1$H} NMR ($C_6D_6$): δ 93.3 (br s). IR (KBr, $\nu_{NN}$) 2006 cm$^{-1}$, IR (THF, $\nu_{NN}$) 2005 cm$^{-1}$, IR (neat, ATR, $\nu_{NN}$) 2003 cm$^{-1}$. Anal. Calcd. for $C_{25}H_{45}N_2OP_2Co$: C, 58.82; H, 8.88; N, 5.49. Found: C, 58.87; H, 8.96; N, 2.95. The slightly low content of nitrogen is considered to be due to the labile property of the coordinated dinitrogen in **3b**.

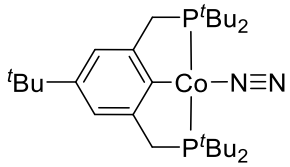


**3c**

**3c**: 41% yield. Purple crystals. Single crystals of **3c** suitable for X-ray crystallography were obtained as purple crystals from hexane at –30 ºC. $^1$H NMR ($C_6D_6$): δ 7.10 (s, 2H), 3.25 (t, *J* = 3.2 Hz, 4H), 1.37 (s, 9H), 1.37 (t, *J* = 6.0 Hz, 36H). $^{31}$P{$^1$H} NMR ($C_6D_6$): δ 92.2 (br s). IR (KBr, $\nu_{NN}$) 2004 cm$^{-1}$, IR (THF, $\nu_{NN}$) 2006 cm$^{-1}$, IR (neat, ATR, $\nu_{NN}$) 2001 cm$^{-1}$. Anal. Calcd. for $C_{28}H_{51}N_2P_2Co$: C, 62.67; H, 9.58; N, 5.22. Found: C, 62.92; H, 9.48; N, 5.03.

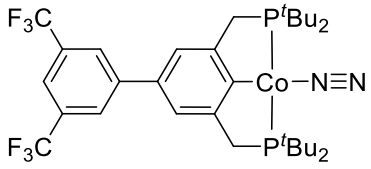


**3d**

**3d**: 41% yield. Purple crystals. $^1$H NMR ($C_6D_6$): δ 7.98 (s, 2H), 7.73 (s, 1H), 6.93 (s, 2H), 3.11 (t, *J* = 3.8 Hz, 4H), 1.37 (t, *J* = 6.0 Hz, 36H). $^{31}$P{$^1$H} NMR ($C_6D_6$): δ 93.3 (s). $^{19}$F NMR ($C_6D_6$): δ -62.5(s). IR (KBr, $\nu_{NN}$) 2009 cm$^{-1}$, IR (THF, $\nu_{NN}$) 2014 cm$^{-1}$, IR (neat, ATR, $\nu_{NN}$) 2005 cm$^{-1}$. Anal. Calcd. for $C_{32}H_{45}N_2F_6P_2Co$: C, 55.49; H, 6.55; N, 4.04. Found: C, 55.51; H, 6.42; N, 3.27. The slightly low content of nitrogen is considered to be due to the labile property of the coordinated dinitrogen in **3d**.

**Reduction of Complex 3a with K.**

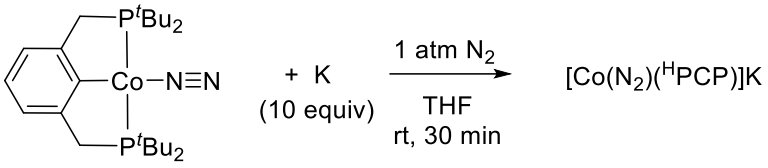


**3a**

A mixture of **3a** (4.8 mg, 10.0 μmol) and potassium (3.9 mg, 100 μmol) in THF (2 mL) was stirred at room temperature for 30 min under $N_2$ (1 atm). After the solvent was removed *in vacuo*, the dark green residue was analyzed by IR. The IR spectrum in KBr shows two absorptions at 2007 $cm^{-1}$ and 1914 $cm^{-1}$. The former is derived from **3a**, while the latter can be assigned as [Co($N_2$)($^H$PCP)]K. During the operation of isolation of the desired complex, the decomposition of complex was observed.

**Catalytic Silylamine Formation from Dinitrogen.**

A typical experimental procedure for catalytic reduction of dinitrogen to silylamine using **3a** is described below. In a 50 mL Schlenk flask were placed **3a** (2.4 mg, 5.0 μmol), $KC_8$ (406 mg, 3.00 mmol). After the addition of $Et_2O$ (6 mL) and $Me_3SiCl$ (380 μL, 3.00 mmol) to the Schlenk, the mixture was stirred at room temperature for 40 h under $N_2$ (1 atm). After dilute $H_2SO_4$ solution (0.5 M, 10 mL) was added to the mixture, the mixture was stirred at room temperature for 1 h. Aqueous solution of KOH (30 wt%, 5 mL) was added to the reaction mixture, and the mixture was distilled into another dilute $H_2SO_4$ solution (0.5 M, 10 mL). The amount of ammonia was determined by the indophenol method.[S7]

Separately, the amount of silylamine and byproducts were determined by GC analysis. A typical experimental procedure is described as below. In a 50 mL Schlenk flask were placed **3a** (2.4 mg, 5.0 μmol), $KC_8$ (406 mg, 3.00 mmol), and cyclododecane (30.0 mg 0.179 mmol) as an internal standard for GC analysis. After the addition of $Et_2O$ (6 mL) and $Me_3SiCl$ (380 μL, 3.00 mmol) to the Schlenk, the mixture was stirred at room temperature for 40 h under $N_2$ (1 atm). An aliquot of the mixture was filtered, and the filtrate was subjected to GC analysis and GC–MS analysis.

The investigations of the optimized reaction conditions were shown in Tables S1–S3. Time profiles of reactions using **3a** and **1** are shown in Figures S1–S2.

**Table S1**. Effect of reductant.

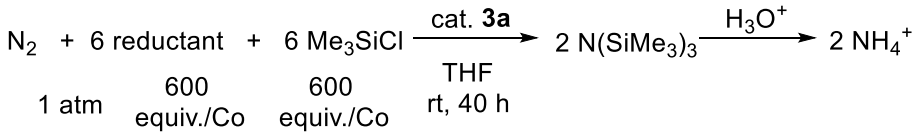


| entry | reductant | $NH_3$ (equiv./Co) |
|---|---|---|
| 1 | Na | 16 |
| 2 | $KC_8$ | 41 |

**Table S2**. Effect of solvent.

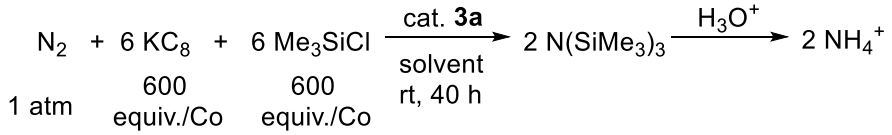


| entry | solvent | $NH_3$ (equiv./Co) |
|---|---|---|
| 1 | THF | 41 |
| 2 | hexane | 23 |
| 3 | $Et_2O$ | 44±3[a] |

[a]Average of 4 runs.

**Table S3**. Effect of temperature.

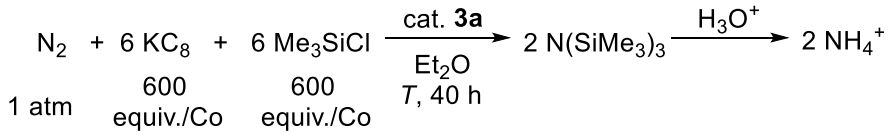


| entry | *T* | $NH_3$ (equiv./Co) |
|---|---|---|
| 1 | –20 °C | 30 |
| 2 | rt | 44±3[a] |

[a]Average of 4 runs.

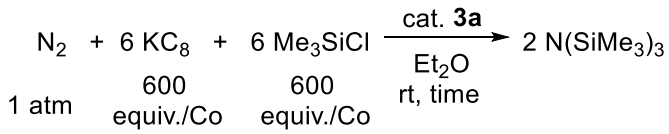


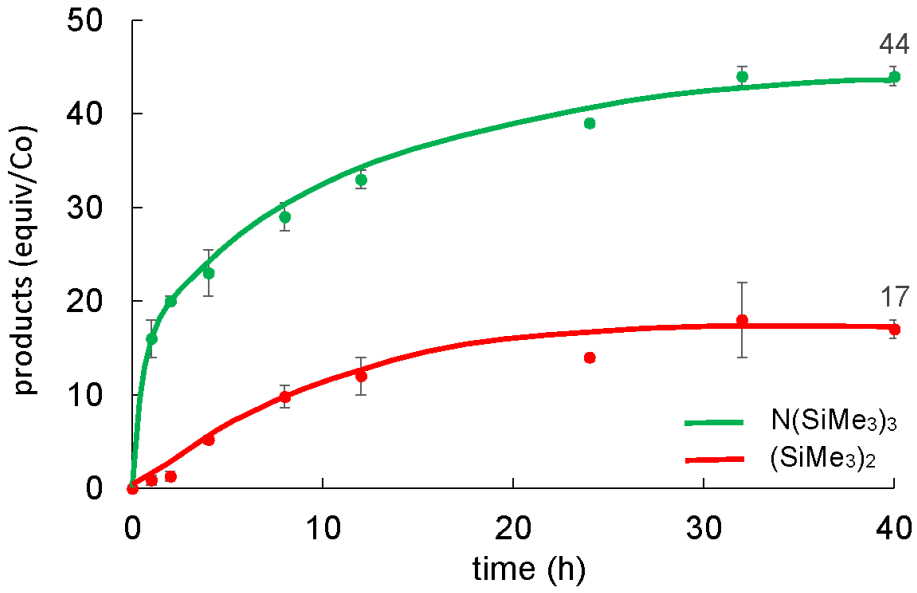


**Figure S1**. Time profile of the reaction using **3a** as a catalyst.

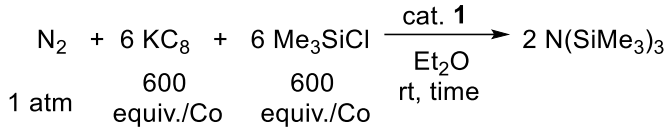


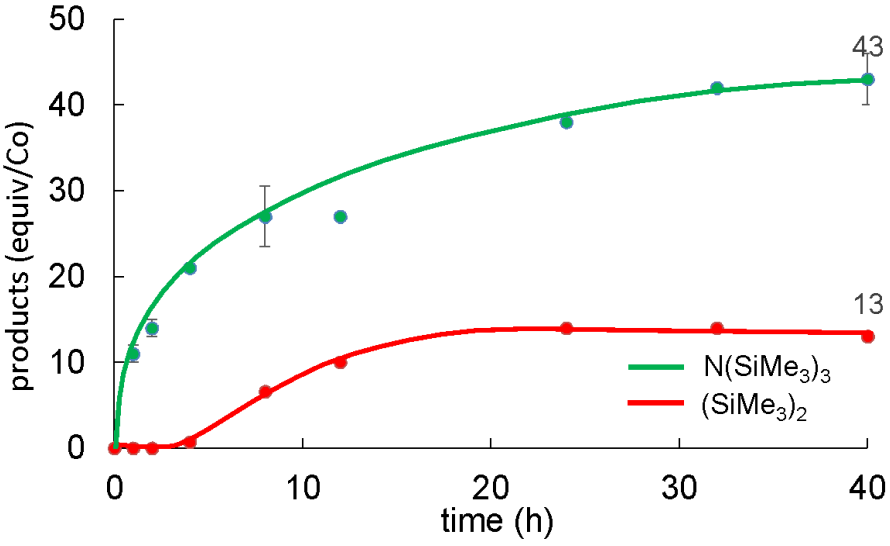


**Figure S2**. Time profile of the reaction using **1** as a catalyst.

**Catalytic Silylamine Formation with Larger Amounts of $KC_8$ and $Me_3SiCl$.**

A typical experimental procedure for catalytic reduction of dinitrogen to silylamine

using **3a** is described below. In a 50 mL Schlenk flask were placed $KC_8$ (406 mg, 3.00 mmol). $Et_2O$ (6 mL), $Me_3SiCl$ (380 μL, 3.00 mmol), and a solution of **3a** (1.0 mM in $Et_2O$, 500 μL, 0.50 μmol) were added, and the mixture was stirred at room temperature for 40 h under $N_2$ (1 atm). After dilute $H_2SO_4$ solution (0.5 M, 10 mL) was added to the mixture, the mixture was stirred at room temperature for 1 h. Aqueous solution of KOH (30 wt%, 5 mL) was added to the reaction mixture, and the mixture was distilled into another dilute $H_2SO_4$ solution (0.5 M, 10 mL). The amount of ammonia was determined by the indophenol method.[S7] The investigation of the effect of the amounts of $KC_8$ and $Me_3SiCl$ was shown in Table S4. Screening of catalysts is shown in Table S5.

**Table S4**. Effect of amounts of $KC_8$ and $Me_3SiCl$.

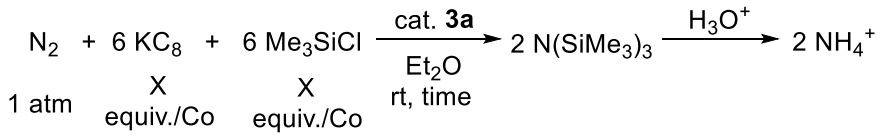


| entry | X | time (h) | $NH_3$ (equiv./Co) |
|---|---|---|---|
| 1 | 600 | 40 | 44±3[a] |
| 2 | 1800 | 40 | 166 |
| 3 | 6000 | 40 | 316±37[b] |
| 4 | 6000 | 96 | 351±42[c] |

[a]Average of 4 runs.
[b]Average of 5 runs.
[c]Average of 3 runs.

**Table S5**. Catalytic reaction of dinitrogen into silylamine using **1** and **3a–3d**.

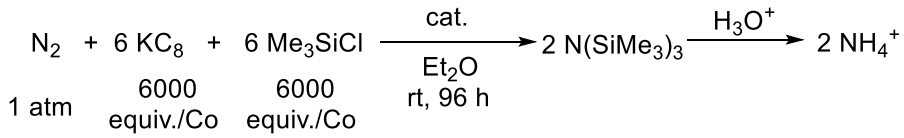


| entry | cat. | $NH_3$ (equiv./Co) |
|---|---|---|
| 1 | **3a** | 351±42[a] |
| 2 | **3b** | 332±23[a] |
| 3 | **3c** | 371±2[b] |
| 4 | **3d** | 106±4[b] |
| 5 | **1** | 353±41[a] |

[a]Average of 3 runs.
[b]Average of 2 runs.

**Further addition of $Me_3SiCl$ and $KC_8$ in Catalytic Silylamine Formation**.

In a 50 mL Schlenk flask were placed **3a** (2.4 mg, 5.0 μmol), $KC_8$ (406 mg, 3.00 mmol), and cyclododecane (30.0 mg 0.179 mmol) as an internal standard for GC analysis. After the addition of $Et_2O$ (6 mL) and $Me_3SiCl$ (380 μL, 3.00 mmol) to the Schlenk, the mixture was stirred at room temperature for 40 h under $N_2$ (1 atm). An aliquot of the mixture was filtered, and the filtrate was subjected to GC analysis to give 43 equiv of $N(SiMe_3)_3$ based on the cobalt atom. After a further addition of $Me_3SiCl$ (380 μL, 3.00 mmol) and suspension of $KC_8$ (406 mg, 3.00 mmol) in $Et_2O$ (6 mL), the resulted suspension was stirred at room temperature under $N_2$ (1 atm) for another 40 h. After dilute $H_2SO_4$ solution (0.5 M, 10 mL) was added to the mixture, the mixture was stirred at room temperature for 1 h. Aqueous solution of KOH (30 wt%, 5 mL) was added to the reaction mixture, and the mixture was distilled into another dilute $H_2SO_4$ solution (0.5 M, 10 mL). The amount of ammonia was determined by the indophenol method.[S7] In total, 44 equiv of $NH_3$ was obtained based on the cobalt atom (Figure S3).

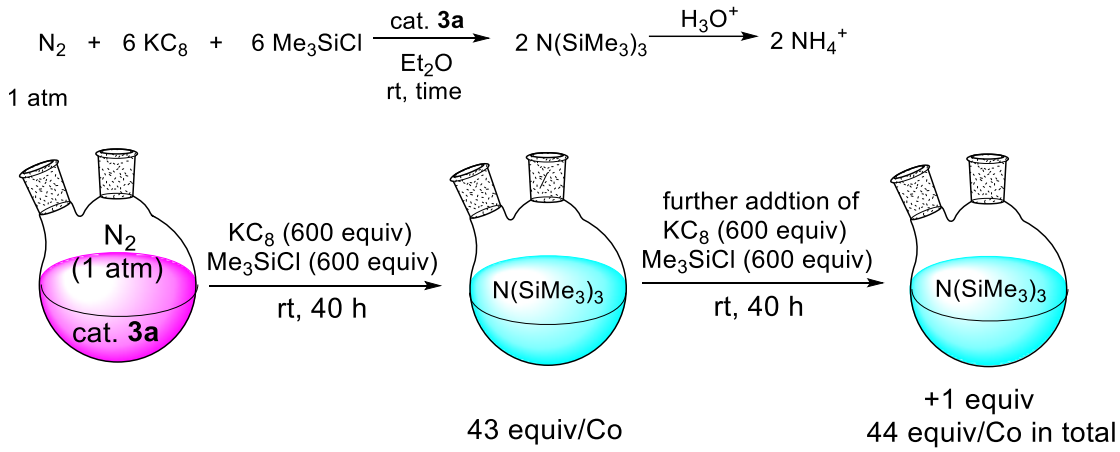


**Figure S3**. Further addition of $Me_3SiCl$ and $KC_8$ in catalytic silylamine formation.

**X-ray Crystallography.**

Crystallographic data of **2a**, **2b**, **2d**, and **3a–3d** are summarized in Tables S6–S9. ORTEP drawings of **2a**, **2b**, **2d**, and **3a–3d** are shown in Figures S4-S10. Diffraction data for **2a**, **2b**, **2d**, and **3a–3d** were collected for the $2\theta$ range of 4° to 60° at –180 °C on a Rigaku XtaLAB Synergy imaging plate area detector with multi-layer mirror monochromated Mo-K$\alpha$ ($\lambda$ = 0.71073 Å) radiation with VariMax optics. Intensity data were corrected for Lorentz and polarization effects and for empirical absorptions (CrysAlisPro[S8]), while structure solutions and refinements were carried out by using *CrystalStructure* package.[S9] The positions of non-hydrogen atoms were determined by direct methods (SHELXS version 2013/1[S10] for **2b**, **3a**, and **3b**; SHELXT version 2014/5[S11] for **2a**, **2d**, **3c**, and **3d**) and subsequent Fourier syntheses (SHELXL[S12] version 2016/6) and were refined on $F_o^2$ using all unique reflections by full-matrix least-squares with anisotropic thermal parameters. All the hydrogen atoms were placed at the calculated positions with fixed isotropic parameters.

In addition, a unit cell of **2a** contains solvent accessible voids of 738 Å$^3$. The difference Fourier maps have suggested that the voids of the crystal were occupied by hexane molecules, which could not be located appropriately because of heavy disorders. Thus, the electron density associated with the solvent molecules was removed by the SQUEEZE routine of PLATONS[S13] for crystal data of **2a**. Crystals of **2a** are efflorescent, loosing hexanes when dried *in vacuo*. Crystal of **3a** contains an inverted structure as a disorder, which was solved as merohedral twins.

**Table S6**. X-ray crystallographic data for **2a**, and **2b**.

| Compound | **2a** | **2b** |
|---|---|---|
| chemical formula | $C_{24}H_{43}BrCoP_2$ | $C_{25}H_{45}BrCoOP_2$ |
| CCDC number | 2097316 | 2122587 |
| formula weight | 532.39 | 562.41 |
| dimensions of crystals, $mm^3$ | 0.552 × 0.162 × 0.070 | 0.466 × 0.350 × 0.347 |
| crystal color, habit | yellow, block | orange, block |
| crystal system | hexagonal | monoclinic |
| space group | $P6_122$ (#178) | $P2_1/n$ (#14) |
| *a*, Å | 16.3648(5) | 15.4207(3) |
| *b*, Å | 16.3648(5) | 11.4009(2) |
| *c*, Å | 19.3030(8) | 31.0696(6) |
| *α*, deg | 90 | 90 |
| *β*, deg | 90 | 92.0009(19) |
| *γ*, deg | 120 | 90 |
| *V*, $Å^3$ | 4476.9 | 5459.01(18) |
| *Z* | 8 | 8 |
| $\rho_{calcd}$, $g \cdot cm^{-3}$ | 1.580 | 1.369 |
| *F*(000) | 2232.00 | 2360.00 |
| $\mu$, $cm^{-1}$ | 27.098 | 22.289 |
| trans. factors range | 0.287–1.000 | 0.167–0.461 |
| no. reflections measured | 41385 | 45917 |
| no. unique reflections | 4139 ($R_{int}$ = 0.0721) | 13394 ($R_{int}$ = 0.0891) |
| no. parameters refined | 135 | 567 |
| *R*1 ($I > 2\sigma(I)$)[a] | 0.0353 | 0.0633 |
| *wR2* (all data)[b] | 0.0877 | 0.1457 |
| GOF[c] | 1.037 | 1.000 |
| flack parameter | –0.018(5) | |
| max diff peak/hole, e $Å^{-3}$ | +0.79/–0.27 | +1.45/–1.21 |

[a] $R1 = \Sigma||F_o|-|F_c||/\Sigma|F_o|$. [b] $wR2 = [\Sigma w(F_o^2-F_c^2)^2/\Sigma w(F_o^2)^2]^{1/2}$, $w = 1/[\sigma^2(F_o^2) + (qP)^2 + rP]$, $P = (\mathrm{Max}(F_o^2, 0) + 2F_c^2)/3$ [$q$ = 0.0556 (**2a**), 0 (**2b**); $r$ = 0 (**2a**), 36.9 (**2b**)]. [c] $\mathrm{GOF} = [\Sigma w(F_o^2-F_c^2)^2/(N_o-N_{params})]^{1/2}$.

**Table S7**. X-ray crystallographic data for **2d** and **3a**.

| compound | **2d** | **3a** |
|---|---|---|
| chemical formula | $C_{32}H_{45}BrCoF_6P_2$ | $C_{24}H_{43}N_2CoP_2$ |
| CCDC number | 2122588 | 2097317 |
| formula weight | 744.48 | 480.50 |
| dimensions of crystals, $mm^3$ | 0.202 × 0.117 × 0.076 | 0.400 × 0.300 × 0.100 |
| crystal color, habit | yellow, block | purple, block |
| crystal system | monoclinic | monoclinic |
| space group | $P2_1/c$ (#14) | $P2_1/c$ (#14) |
| *a*, Å | 7.7639(5) | 45.7720(5) |
| *b*, Å | 14.4515(8) | 14.95170(13) |
| *c*, Å | 29.5341(17) | 15.22530(14) |
| *α*, deg | 90 | 90 |
| *β*, deg | 96.567(5) | 91.4774(9) |
| *γ*, deg | 90 | 90 |
| *V*, $Å^3$ | 3292.0(3) | 10416.26(17) |
| *Z* | 4 | 16 |
| $\rho_{calcd}$, $g\cdot cm^{-3}$ | 1.502 | 1.226 |
| *F*(000) | 1532.00 | 4128.00 |
| $\mu$, $cm^{-1}$ | 18.914 | 7.947 |
| trans. factors range | 0.746–0.866 | 0.620–0.924 |
| no. reflections measured | 28358 | 272797 |
| no. unique reflections | 8345 ($R_{int}$ = 0.1481) | 28620 ($R_{int}$ = 0.0008) |
| no. parameters refined | 391 | 1094 |
| *R*1 ($I > 2\sigma(I)$)[a] | 0.0854 | 0.0891 |
| *wR2* (all data)[b] | 0.1766 | 0.2153 |
| GOF[c] | 1.015 | 1.075 |
| max diff peak/hole, e $Å^{-3}$ | +0.96/–0.84 | +2.13/–1.47 |

[a] $R1 = \Sigma||F_o|-|F_c||/\Sigma|F_o|$. [b] $wR2 = [\Sigma w(F_o^2-F_c^2)^2/\Sigma w(F_o^2)^2]^{1/2}$, $w = 1/[\sigma^2(F_o^2) + (qP)^2 + rP]$, $P = (\mathrm{Max}(F_o^2, 0) + 2F_c^2)/3$ [$q$ = 0.0674 (**2d**), 0 (**3a**); $r$ = 3.1383 (**2d**), 160 (**3a**)]. [c] $GOF = [\Sigma w(F_o^2-F_c^2)^2/(N_o-N_{params})]^{1/2}$.

**Table S8**. X-ray crystallographic data for **3a** and **3c**.

| compound | **3b** | **3c** |
|---|---|---|
| chemical formula | $C_{25}H_{45}N_2CoOP_2$ | $C_{28}H_{51}N_2CoP_2$ |
| CCDC number | 2122589 | 2122590 |
| formula weight | 510.52 | 536.61 |
| dimensions of crystals, $mm^3$ | 0.514 × 0.086 × 0.054 | 0.507 × 0.379 × 0.260 |
| crystal color, habit | purple, needle | purple, block |
| crystal system | monoclinic | monoclinic |
| space group | $P2_1/n$ (#14) | $P2_1/n$ (#14) |
| *a*, Å | 15.2809(5) | 15.1643(6) |
| *b*, Å | 11.3641(3) | 11.6686(4) |
| *c*, Å | 31.2253(9) | 17.1444(6) |
| *α*, deg | 90 | 90 |
| *β*, deg | 91.929(3) | 102.770(4) |
| *γ*, deg | 90 | 90 |
| *V*, $Å^3$ | 5419.3(3) | 2958.60(19) |
| *Z* | 8 | 4 |
| $\rho_{calcd}$, $g \cdot cm^{-3}$ | 1.251 | 1.205 |
| *F*(000) | 2192.00 | 1160.00 |
| $\mu$, $cm^{-1}$ | 7.704 | 7.064 |
| trans. factors range | 0.124–1.000 | 0.126–0.832 |
| no. reflections measured | 49088 | 21907 |
| no. unique reflections | 14708 ($R_{int}$ = 0.0956) | 7856 ($R_{int}$ = 0.1124) |
| no. parameters refined | 585 | 313 |
| *R*1 ($I > 2\sigma(I)$)[a] | 0.0680 | 0.0775 |
| *wR2* (all data)[b] | 0.1743 | 0.2098 |
| GOF[c] | 1.001 | 1.009 |
| max diff peak/hole, e $Å^{-3}$ | +1.48/–1.01 | +1.39/–0.65 |

[a] $R1 = \Sigma||F_o|-|F_c||/\Sigma|F_o|$. [b] $wR2 = [\Sigma w(F_o^2-F_c^2)^2/\Sigma w(F_o^2)^2]^{1/2}$, $w = 1/[\sigma^2(F_o^2) + (qP)^2 + rP]$, $P = (\mathrm{Max}(F_o^2, 0) + 2F_c^2)/3$ [$q$ = 0.0845 (**3b**), 0.1024 (**3c**); $r$ = 0 (**3b**), 3.0906 (**3c**)]. [c] $GOF = [\Sigma w(F_o^2-F_c^2)^2/(N_o-N_{params})]^{1/2}$.

**Table S9**. X-ray crystallographic data for **3d**.

| compound | **3d** |
|---|---|
| chemical formula | $C_{32}H_{45}N_2CoF_6P_2$ |
| CCDC number | 2122591 |
| formula weight | 692.59 |
| dimensions of crystals, $mm^3$ | 0.182 × 0.134 × 0.105 |
| crystal color, habit | purple, block |
| crystal system | monoclinic |
| space group | $P2_1/c$ (#14) |
| *a*, Å | 7.7722(3) |
| *b*, Å | 14.4666(6) |
| *c*, Å | 29.5984(13) |
| *α*, deg | 90 |
| *β*, deg | 96.166(4) |
| *γ*, deg | 90 |
| *V*, $Å^3$ | 3308.7(2) |
| *Z* | 4 |
| $\rho_{calcd}$, $g \cdot cm^{-3}$ | 1.390 |
| *F*(000) | 1448.00 |
| $\mu$, $cm^{-1}$ | 6.740 |
| trans. factors range | 0.845 - 0.932 |
| no. reflections measured | 23553 |
| no. unique reflections | 8300 ($R_{int}$ = 0.0366) |
| no. parameters refined | 400 |
| *R*1 ($I > 2\sigma(I)$)[a] | 0.0475 |
| *wR2* (all data)[b] | 0.1188 |
| GOF[c] | 1.015 |
| max diff peak/hole, e $Å^{-3}$ | +1.10/–0.94 |

[a] $R1 = \Sigma||F_o|-|F_c||/\Sigma|F_o|$. [b] $wR2 = [\Sigma w(F_o^2-F_c^2)^2/\Sigma w(F_o^2)^2]^{1/2}$, $w = 1/[\sigma^2(F_o^2) + (qP)^2 + rP]$, $P = (\mathrm{Max}(F_o^2, 0) + 2F_c^2)/3$ [$q$ = 0.0476; $r$ = 5.3030]. [c] $\mathrm{GOF} = [\Sigma w(F_o^2-F_c^2)^2/(N_o-N_{params})]^{1/2}$.

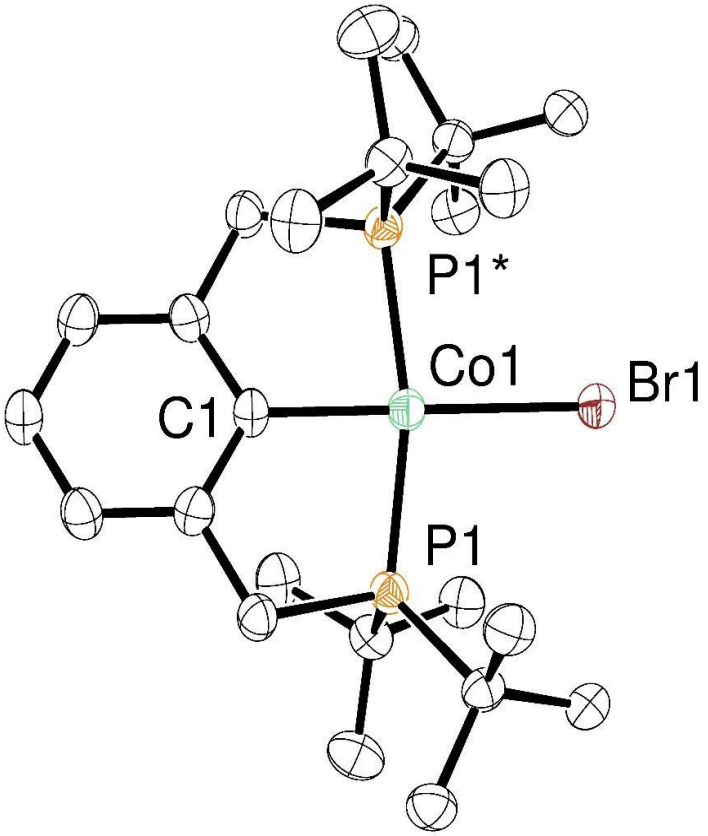


**Figure S4**. Molecular structure of **2a**. Thermal ellipsoids are shown at the 50% probability level. Hydrogen atoms are omitted for clarity. Selected interatomic distances (Å) and angles (deg): Co(1)–P(1) 2.2408(7), Co(1)–C(1) 1.957(3), Co(1)–Br(1) 2.4107(6); P(1)–Co(1)–P(1*) 166.78(4), Br(1)–Co(1)–C(1) 180.00(5).

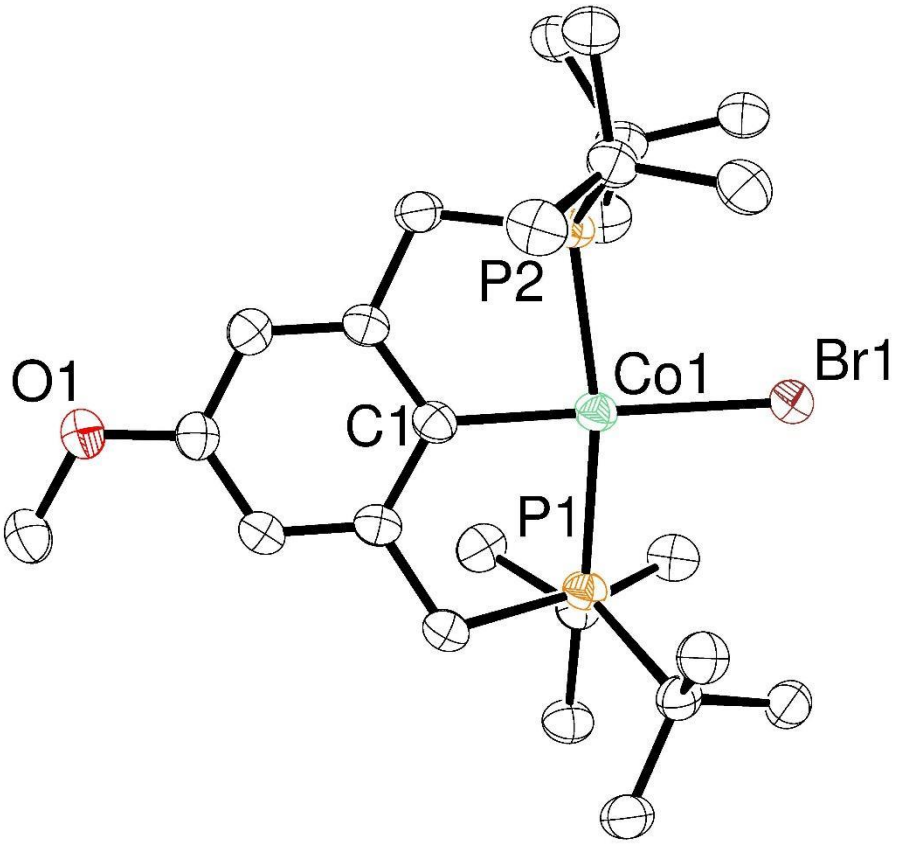


**Figure S5**. Molecular structure of one of the two crystallographically independent molecules **2b**. Thermal ellipsoids are shown at the 50% probability level. Hydrogen atoms are omitted for clarity. Selected interatomic distances (Å) and angles (deg): Co(1)–P(1) 2.2376(13), Co(1)–P(2) 2.2436(13), Co(1)–C(1) 1.964(5), Co(1)–Br(1) 2.3952(8); P(1)–Co(1)–P(2) 165.54(5), Br(1)–Co(1)–C(1) 175.96(13); Co(2)–P(3) 2.2285(12), Co(2)–P(4) 2.2344(13), Co(2)–C(26) 1.957(5), Co(2)–Br(2) 2.3967(8); P(3)–Co(2)–P(4) 168.61(5), Br(2)–Co(2)–C(26) 179.14(13).

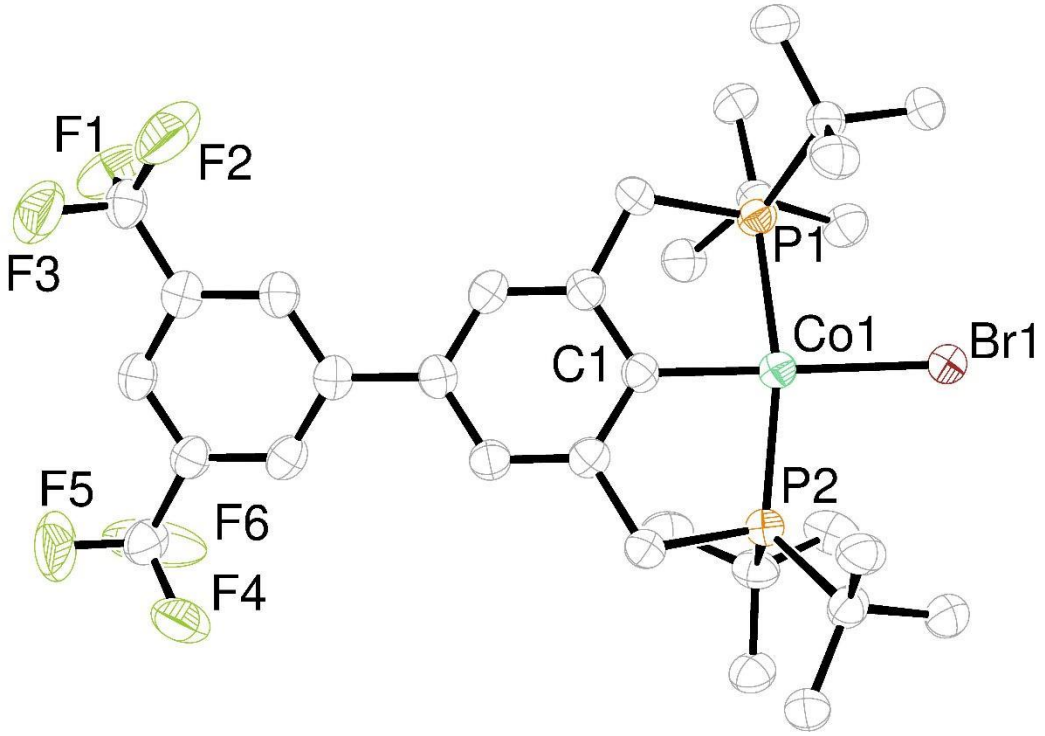


**Figure S6**. Molecular structure of **2d**. Thermal ellipsoids are shown at the 50% probability level. Hydrogen atoms are omitted for clarity. Selected interatomic distances (Å) and angles (deg): Co(1)–P(1) 2.2446(18), Co(1)–P(2) 2.2369(18), Co(1)–C(1) 1.957(6), Co(1)–Br(1) 2.4022(10); P(1)–Co(1)–P(2) 165.43(7), Br(1)–Co(1)–C(1) 173.51(18).

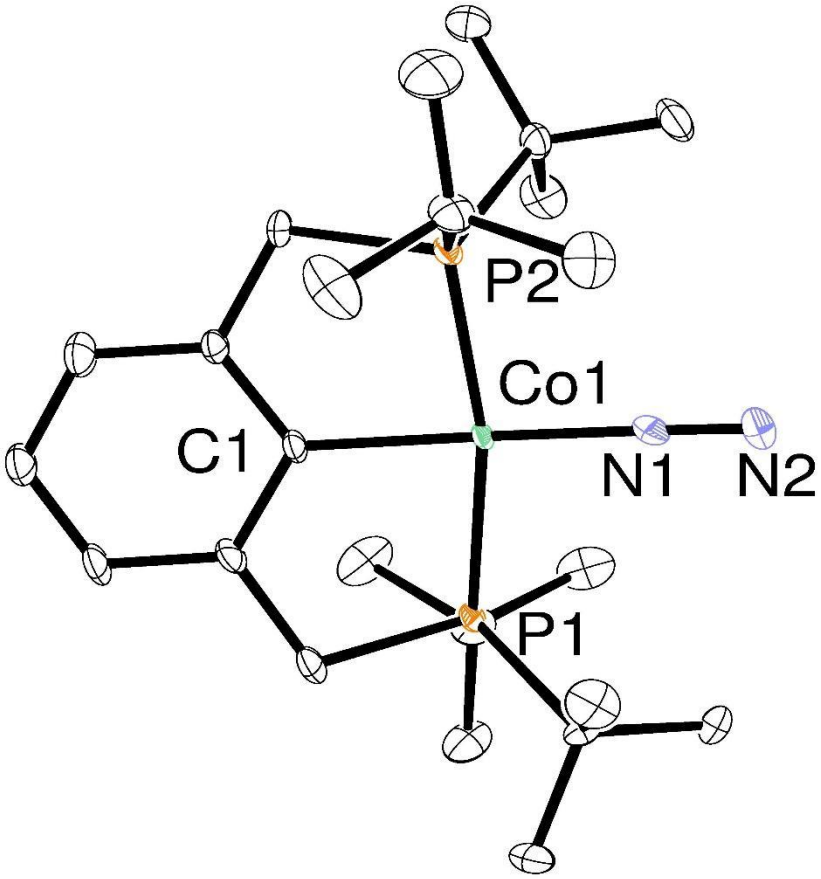


**Figure S7**. Molecular structure of one of the four crystallographically independent molecules **3a**. Thermal ellipsoids are shown at the 50% probability level. Hydrogen atoms are omitted for clarity. Selected interatomic distances (Å) and angles (deg): Co(1)–P(1) 2.1863(17), Co(1)–P(2) 2.1817(17), Co(1)–C(1) 1.959(6), Co(1)–N(1) 1.753(6), N(1)–N(2) 1.115(9); P(1)–Co(1)–P(2) 167.36(7), N(1)–Co(1)–C(1) 174.1(3), Co(1)–N(1)–N(2) 175.6(6); Co(2)–P(3) 2.1897(17), Co(2)–P(4) 2.1928(19), Co(2)–C(25) 1.955(6), Co(2)–N(3) 1.760(5), N(3)–N(4) 1.125(8); P(3)–Co(2)–P(4) 166.57(7), N(3)–Co(2)–C(25) 177.3(2), Co(2)–N(3)–N(4) 178.8(6); Co(3)–P(5) 2.1823(19), Co(3)–P(6) 2.186(2), Co(3)–C(49) 1.966(6), Co(3)–N(5) 1.759(6), N(5)–N(6) 1.138(9); P(5)–Co(3)–P(6) 168.36(8), N(5)–Co(3)–C(49) 178.6(3), Co(3)–N(5)–N(6) 179.2(6); Co(4)–P(7) 2.1793(17), Co(4)–P(8) 2.1876(18), Co(4)–C(73) 1.954(6), Co(4)–N(7) 1.752(6), N(7)–N(8) 1.128(9); P(7)–Co(4)–P(8) 167.82(7), N(7)–Co(4)–C(73) 173.2(3), Co(4)–N(7)–N(8) 175.5(6).

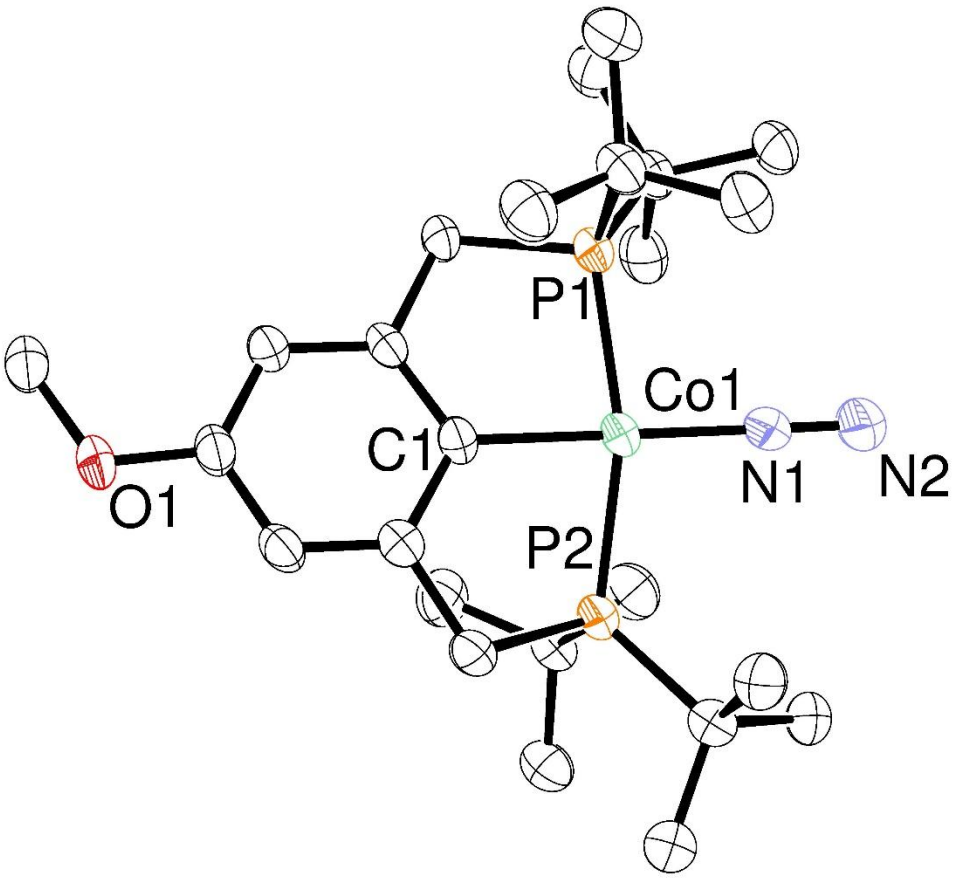


**Figure S8**. Molecular structure of one of the two crystallographically independent molecules **3b**. Thermal ellipsoids are shown at the 50% probability level. Hydrogen atoms are omitted for clarity. Selected interatomic distances (Å) and angles (deg): Co(1)–P(1) 2.1866(10), Co(1)–P(2) 2.1878(9), Co(1)–C(1) 1.961(3), Co(1)–N(1) 1.755(3); N(1)–N(2) 1.106(5); P(1)–Co(1)–P(2) 167.97(4), N(1)–Co(1)–C(1) 178.57(14), Co(1)–N(1)–N(2) 179.3(3); Co(2)–P(3) 2.1941(10), Co(2)–P(4) 2.1995(9), Co(2)–C(26) 1.950(3), Co(2)–N(3) 1.756(3); N(3)–N(4) 1.112(5); P(3)–Co(2)–P(4) 164.03(4), N(3)–Co(2)–C(26) 173.74(14), Co(2)–N(3)–N(4) 177.3(3).

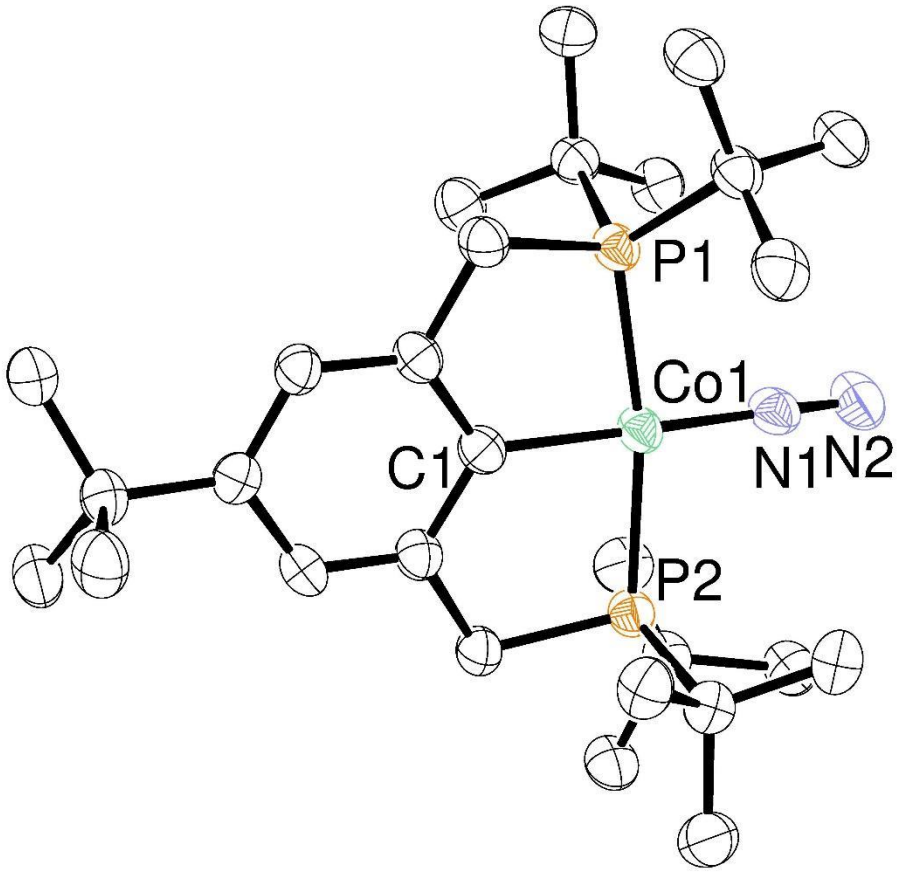


**Figure S9**. Molecular structure of **3c**. Thermal ellipsoids are shown at the 50% probability level. Hydrogen atoms are omitted for clarity. Selected interatomic distances (Å) and angles (deg): Co(1)–P(1) 2.1808(10), Co(1)–P(2) 2.1792(10), Co(1)–C(1) 1.958(4), Co(1)–N(1) 1.751(4); N(1)–N(2) 1.130(5); P(1)–Co(1)–P(2) 168.21(5), N(1)–Co(1)–C(1) 177.73(15), Co(1)–N(1)–N(2) 178.2(3).

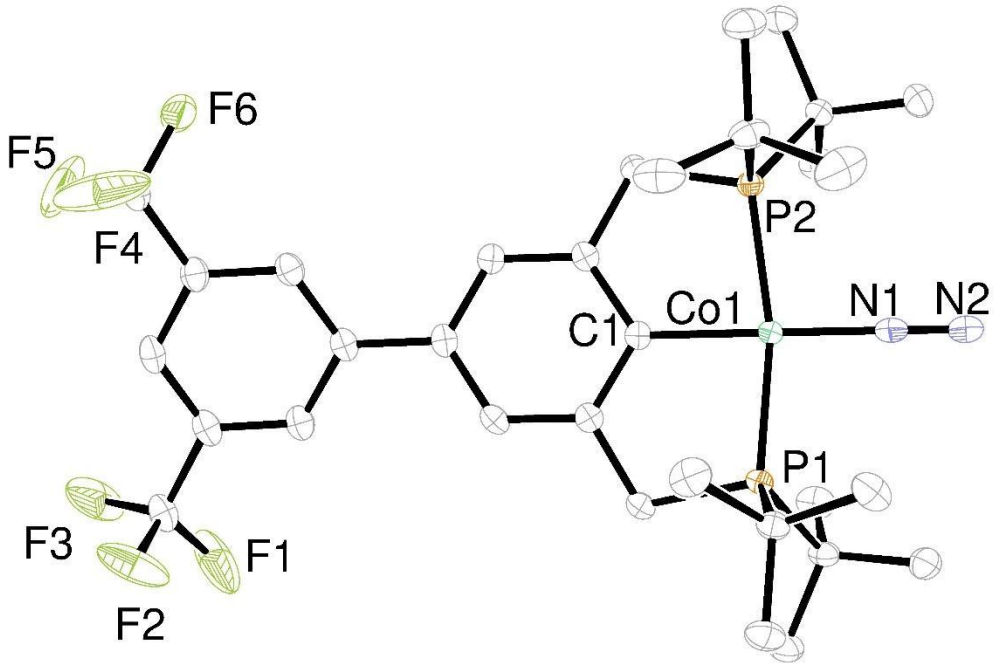


**Figure S10**. Molecular structure of **3d**. Thermal ellipsoids are shown at the 50% probability level. Hydrogen atoms are omitted for clarity. Selected interatomic distances (Å) and angles (deg): Co(1)–P(1) 2.2015(8), Co(1)–P(2) 2.1952(8), Co(1)–C(1) 1.960(2), Co(1)–N(1) 1.767(2), N(1)–N(2) 1.089(3); P(1)–Co(1)–P(2) 164.24(3), N(1)–Co(1)–C(1) 174.27(10), Co(1)–N(1)–N(2) 177.0(2).

**Computational Details.**

Density-functional-theory (DFT) calculations were performed with the Gaussian 09 program (Rev. E01).[S14] All geometry optimizations were carried out with the B3LYP functional with the Grimme's dispersion correction (B3LYP-D3).[S15-19] We employed the SDD (Stuttgart/Dresden pseudopotentials) basis set[S20,21] for Co and the 6-31G(d) basis set[S22-25] for the other atoms, respectively. Solvation effects of THF ($\varepsilon$ = 7.4257) were taken into account by using the polarizable continuum model (PCM)[S26] for all calculations. Optimized structures were confirmed to have no imaginary frequencies by vibrational analysis. Figure S11 presents optimized structures of **3a** and its silylated complexes **I**-**III**, [Co(NN(SiMe$_3$)$_x$)($^{H}$PCP)] ($x$ = 1-3). Figure S12 presents optimized structures of **1**. To discuss the energetics, single-point energy calculations were performed for all optimized structures at the B3LYP-D3/def2-TZVP[S27,28] level of theory. Free energy changes at 298 K ($\Delta G_{298}$) for the silylation are calculated based on reaction [Co(NN(SiMe$_3$)$_{x-1}$)($^{H}$PCP)] + •SiMe$_3$ → [Co(NN(SiMe$_3$)$_x$)($^{H}$PCP)] ($x$ = 1-3), where •SiMe$_3$ represents a trimethylsilyl radical. Detailed data on SCF energies, thermal energy corrections at 298 K, SCF energies in THF are summarized in Table S10.

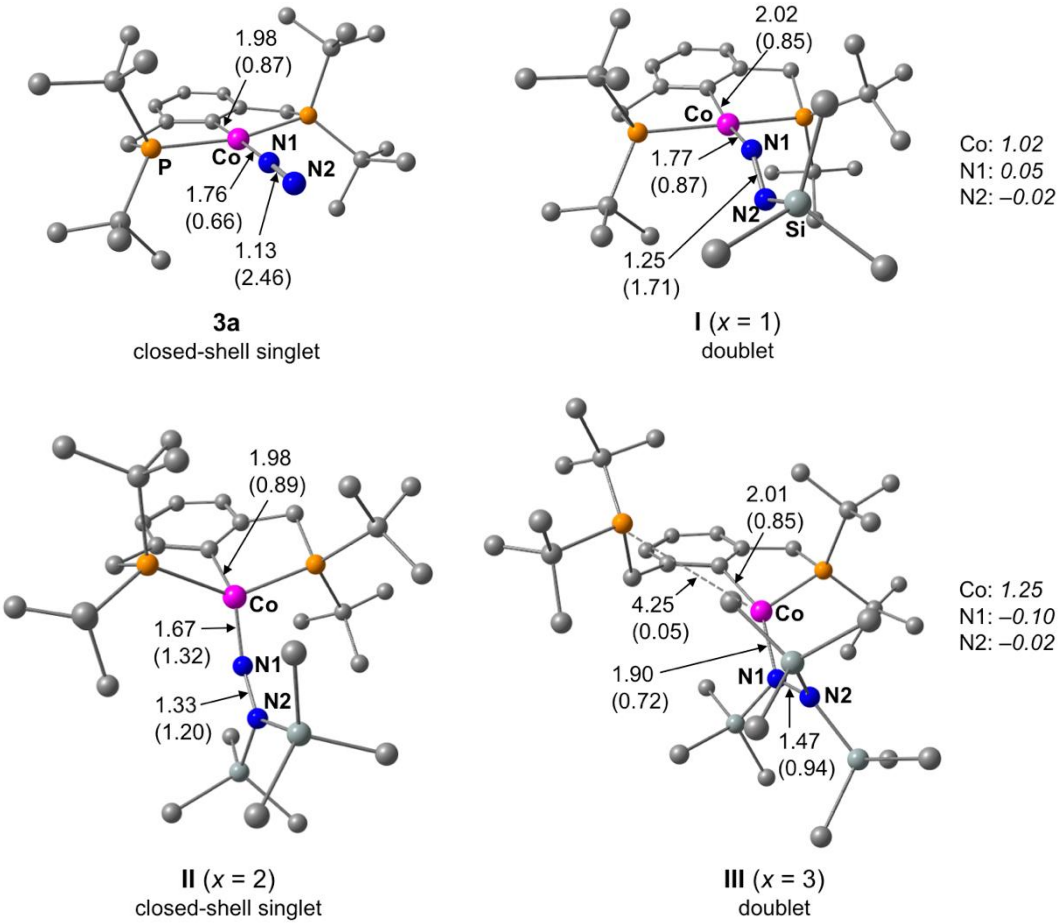


**Figure S11**. Optimized structure and selected geometric parameters of [Co($N_2$)($^{H}$PCP)] **3a** and its silylated complexes [Co(NN($SiMe_3$)$_x$)($^{H}$PCP)] ($x$ = 1-3). Bond distances are presented in Å. Hydrogen atoms are omitted for clarity. The Mulliken spin densities assigned to the Co center and two N atoms are given in italics. The Mayer bond orders are presented in parenthesis.

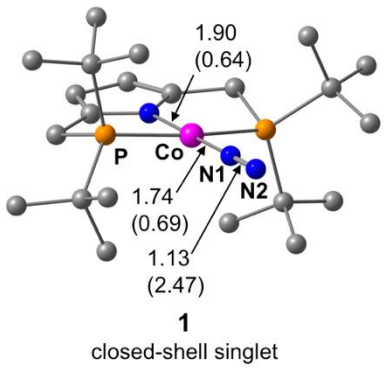


**Figure S12**. Optimized structure and selected geometric parameters of [Co($N_2$)(PNP)] **1**. Bond distances are presented in Å. Hydrogen atoms are omitted for clarity. The Mayer bond orders are presented in parenthesis.

**Table S10**. SCF energies (*in vacuo*), thermal energy corrections at 298 K, SCF enegies in THF.

| Species | SCF energy /hartree | Thermal corrections /hartree | SCF energy (THF) /hartree |
|---|---|---|---|
| **3a** | -1878.67001596 | 0.571365 | -3116.12441083 |
| **1** | -1856.62487600 | 0.554889 | -3094.07385705 |
| **I** | -2287.92085942 | 0.674142 | -3525.45227131 |
| **II** | -2697.19367511 | 0.785825 | -3934.81170635 |
| **III** | -3106.48642047 | 0.887419 | -4344.18338624 |

**NMR and IR Spectra.**

**4**, $^{1}H$ NMR ($CDCl_3$, 400 MHz)

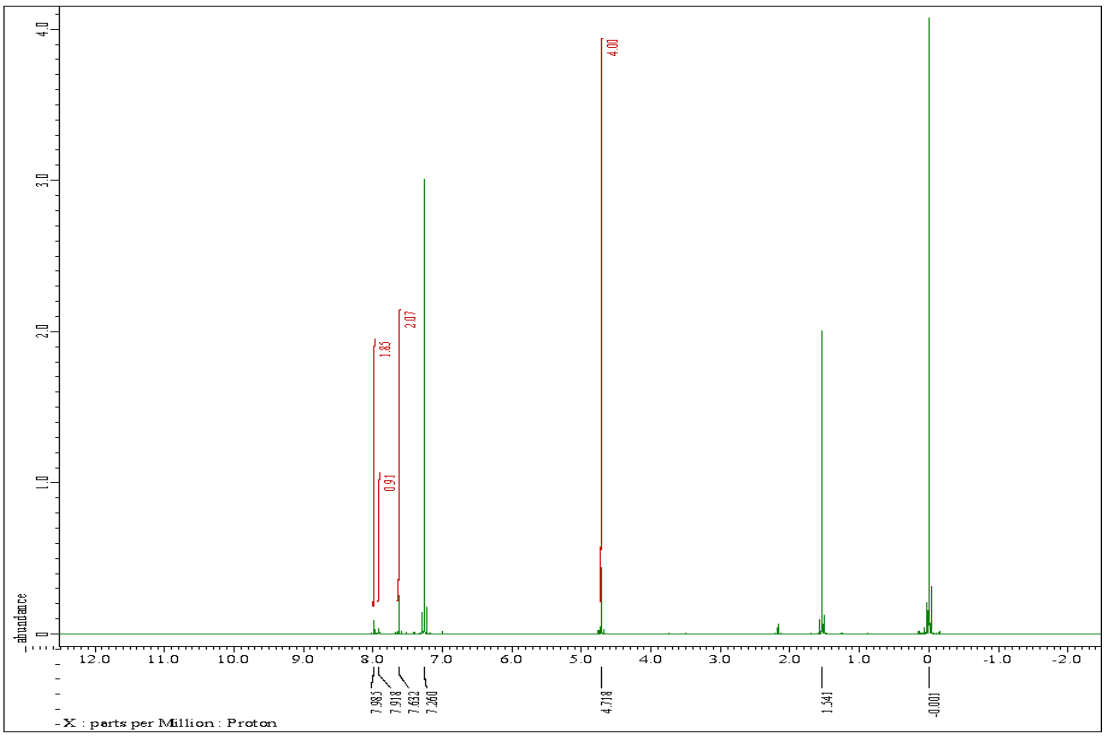


**4**, $^{13}C\{^{1}H\}$ NMR ($CDCl_3$, 100 MHz)

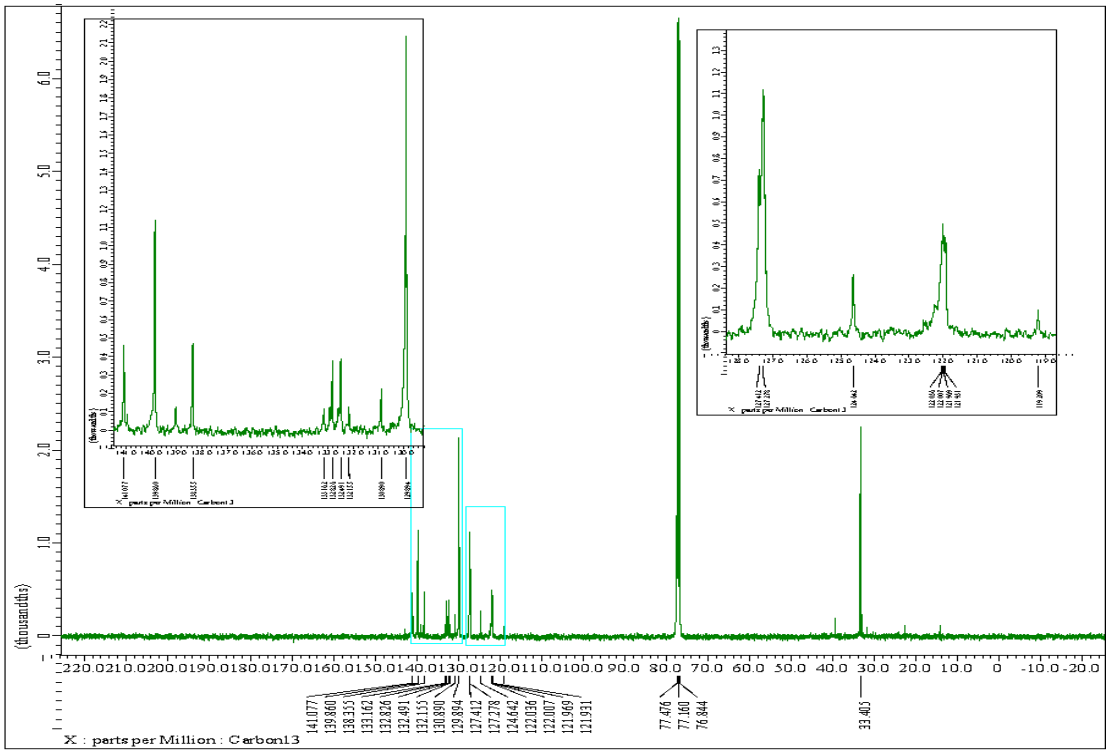

**4**, $^{19}F$ NMR ($CDCl_3$, 376 MHz)

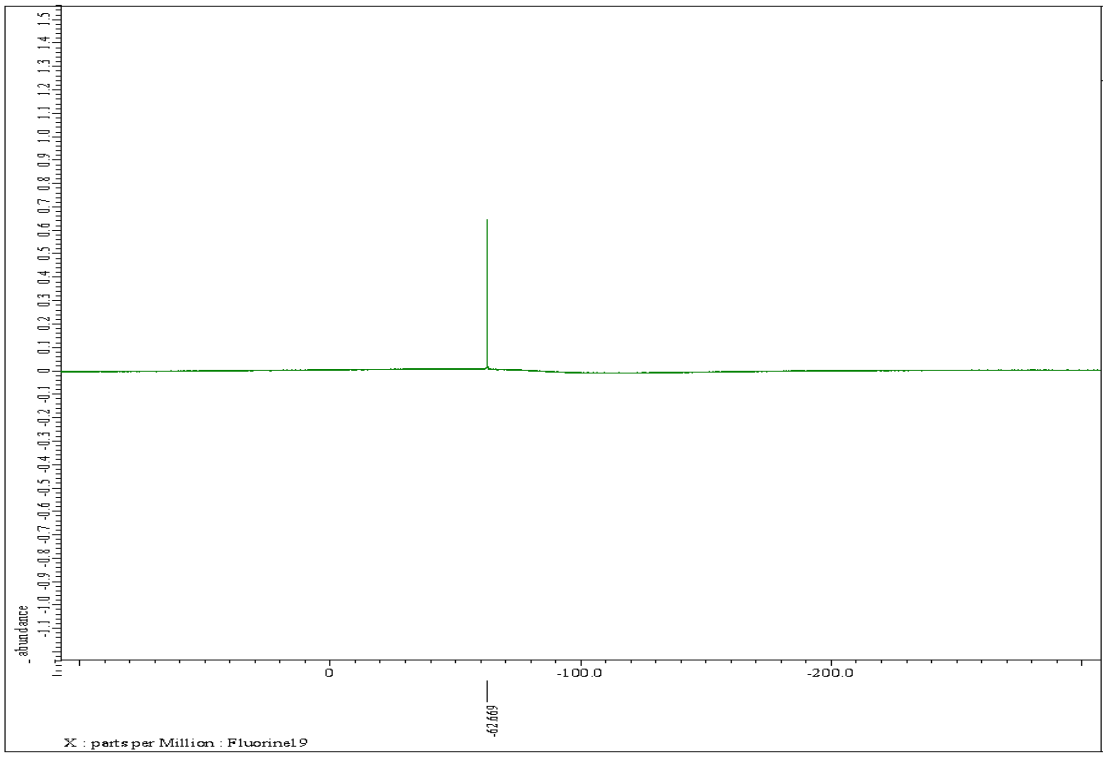

$^{H}$PCP–Br, $^{1}$H NMR ($C_6D_6$, 400 MHz)

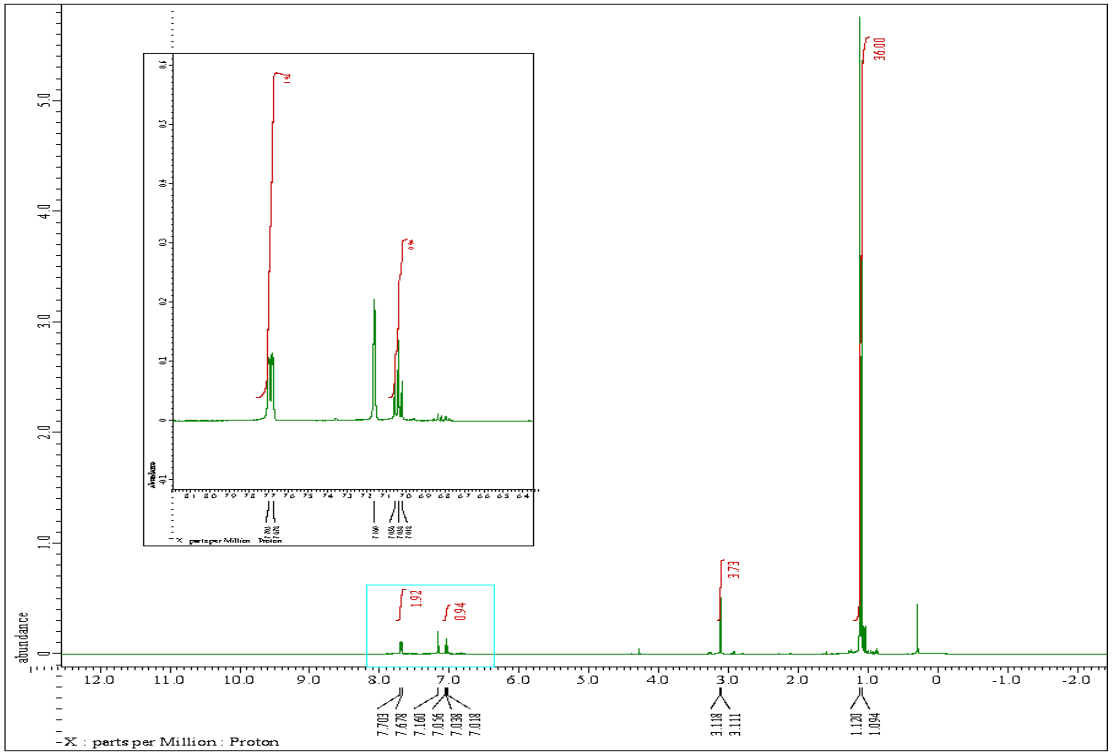


$^{H}$PCP–Br, $^{13}$C{$^{1}$H} NMR ($C_6D_6$, 100 MHz)

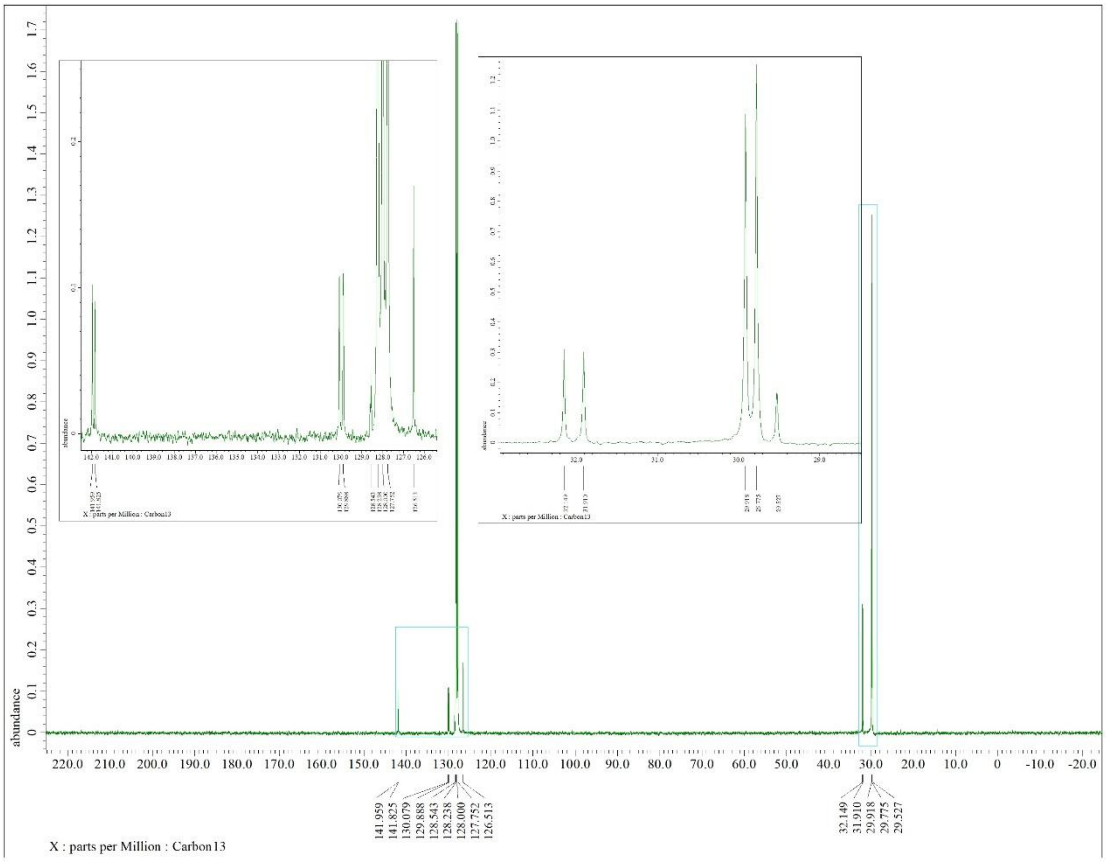

$^{H}$PCP–Br, $^{31}P\{^{1}H\}$ NMR ($C_6D_6$, 162 MHz)

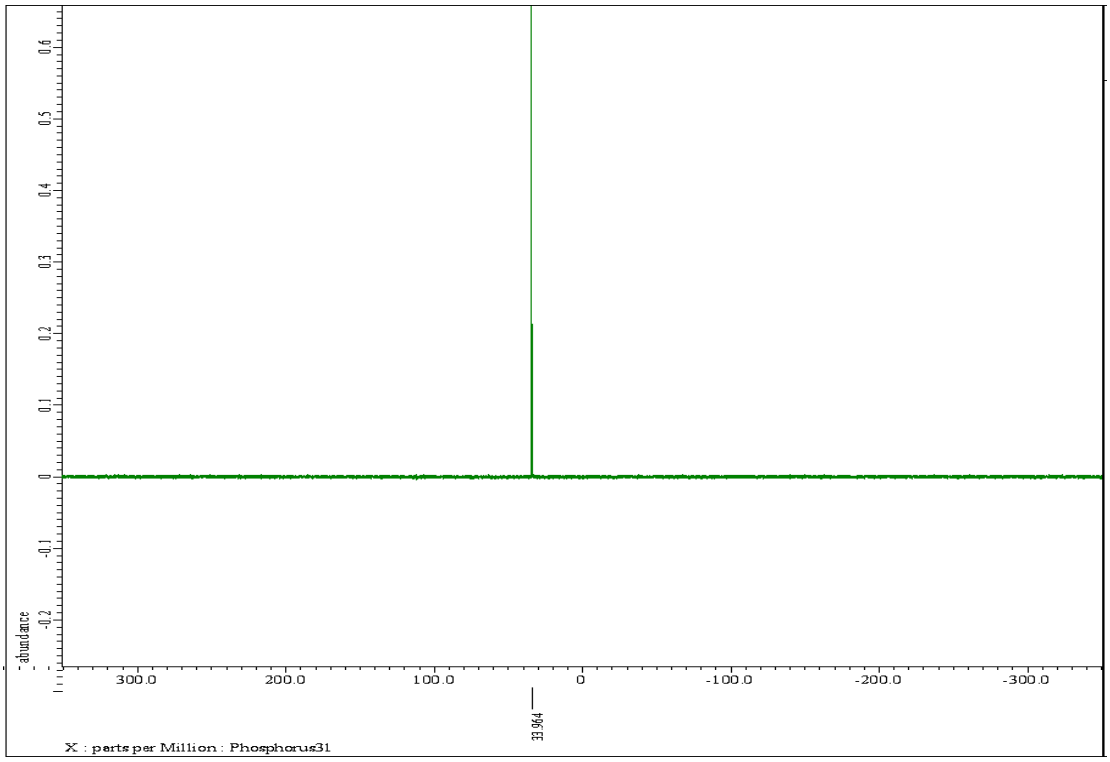

$^{MeO}$PCP–Br, $^{1}$H NMR ($C_6D_6$, 400 MHz)

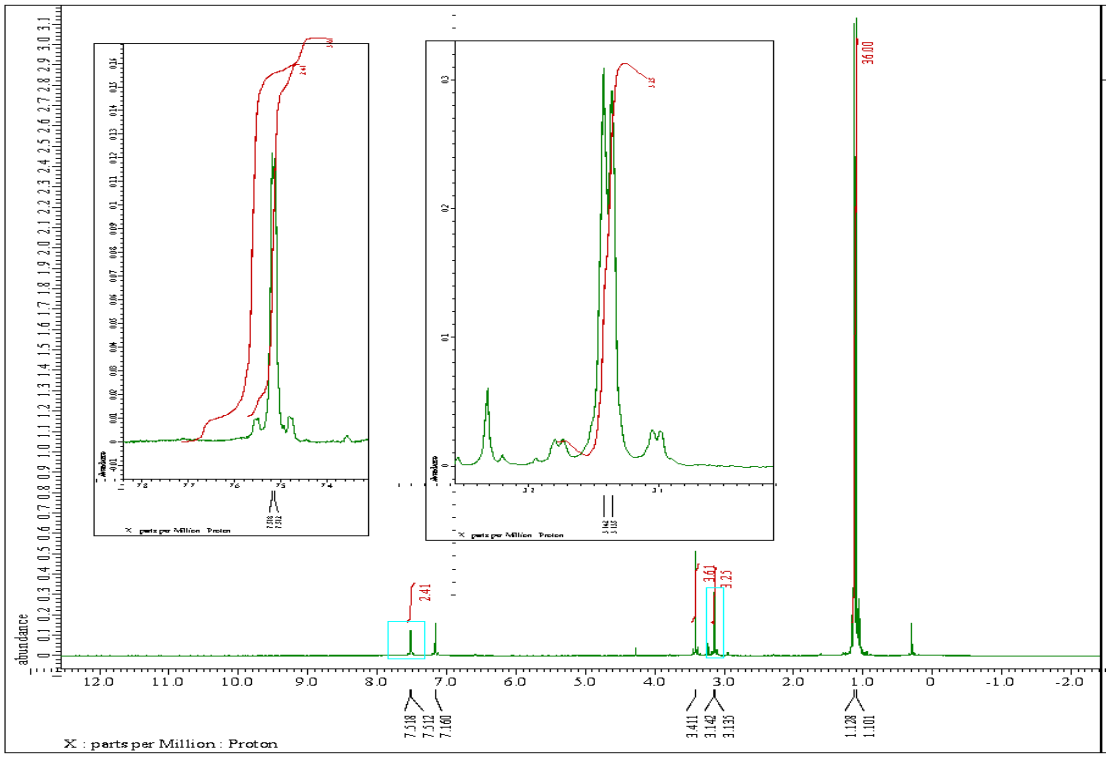


$^{MeO}$PCP–Br, $^{13}$C{$^{1}$H} NMR ($C_6D_6$, 100 MHz)

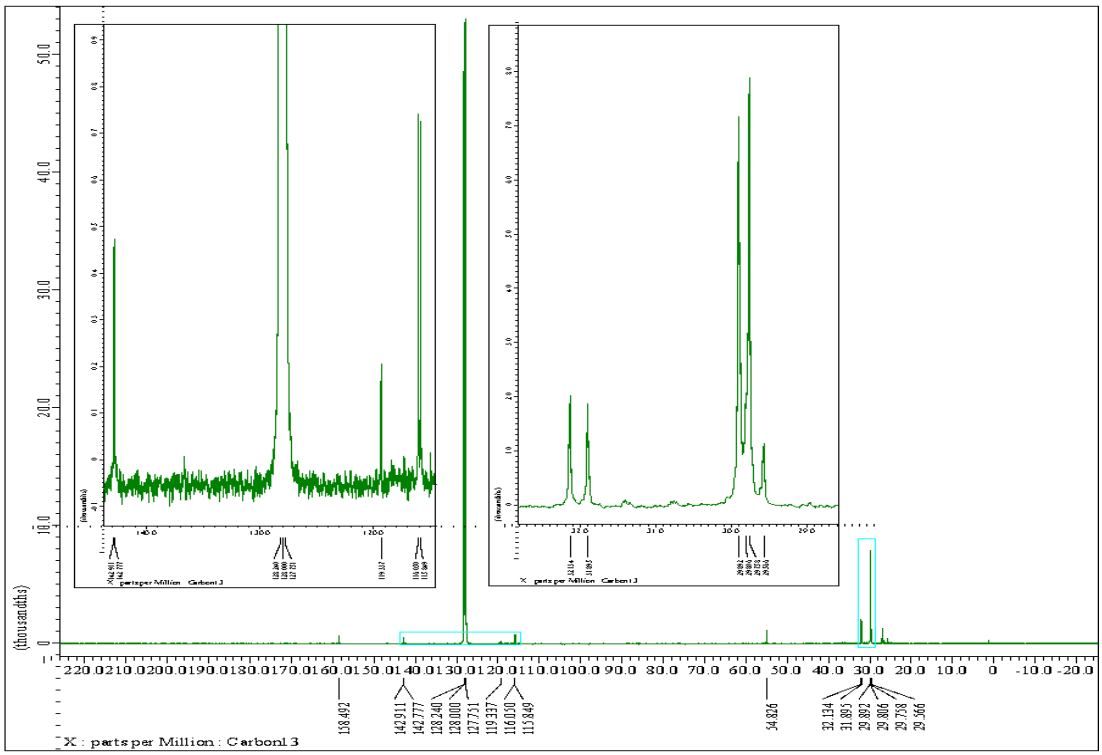

$^{MeO}$PCP–Br, $^{31}P\{^{1}H\}$ NMR ($C_6D_6$, 162 MHz)

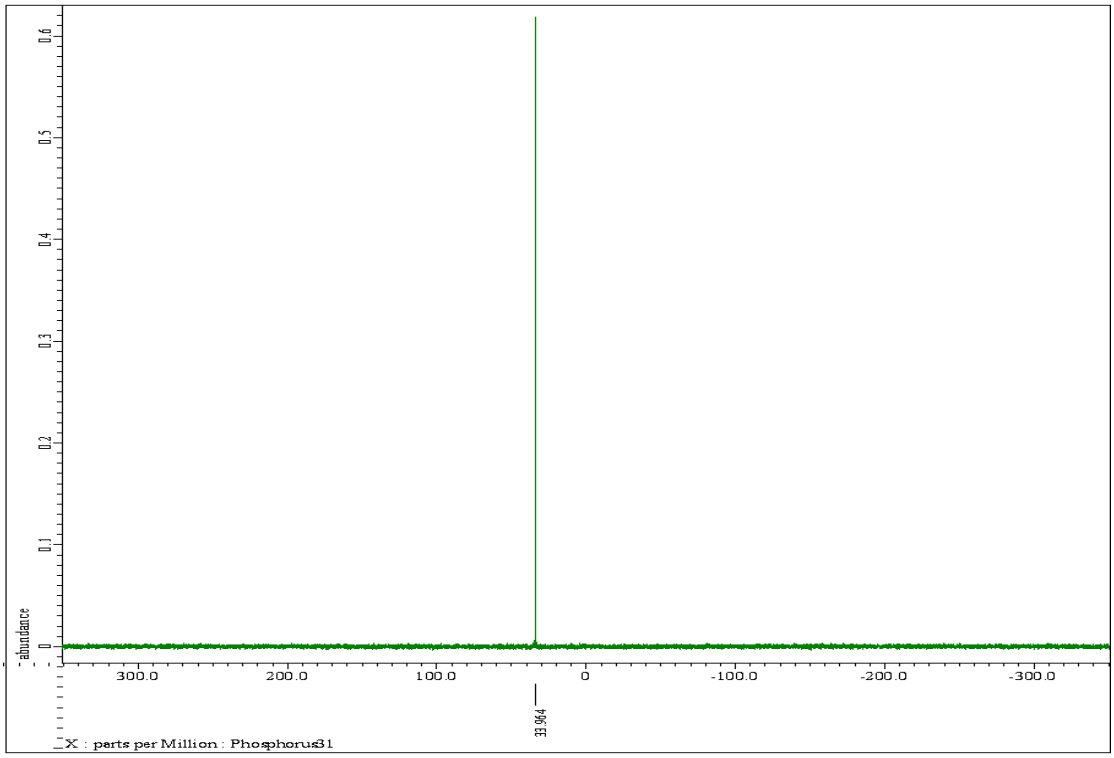

$^{t\text{Bu}}$PCP–Br, $^{1}$H NMR ($C_6D_6$, 400 MHz)

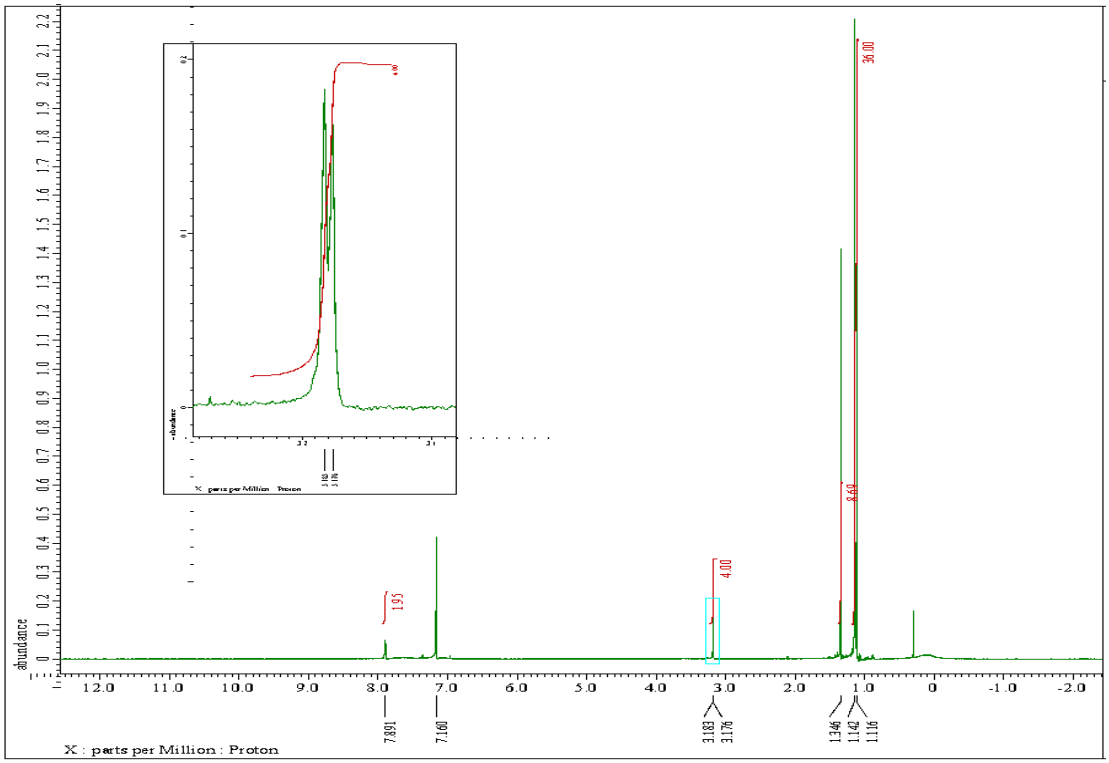


$^{t\text{Bu}}$PCP–Br, $^{13}$C NMR ($C_6D_6$, 100 MHz)

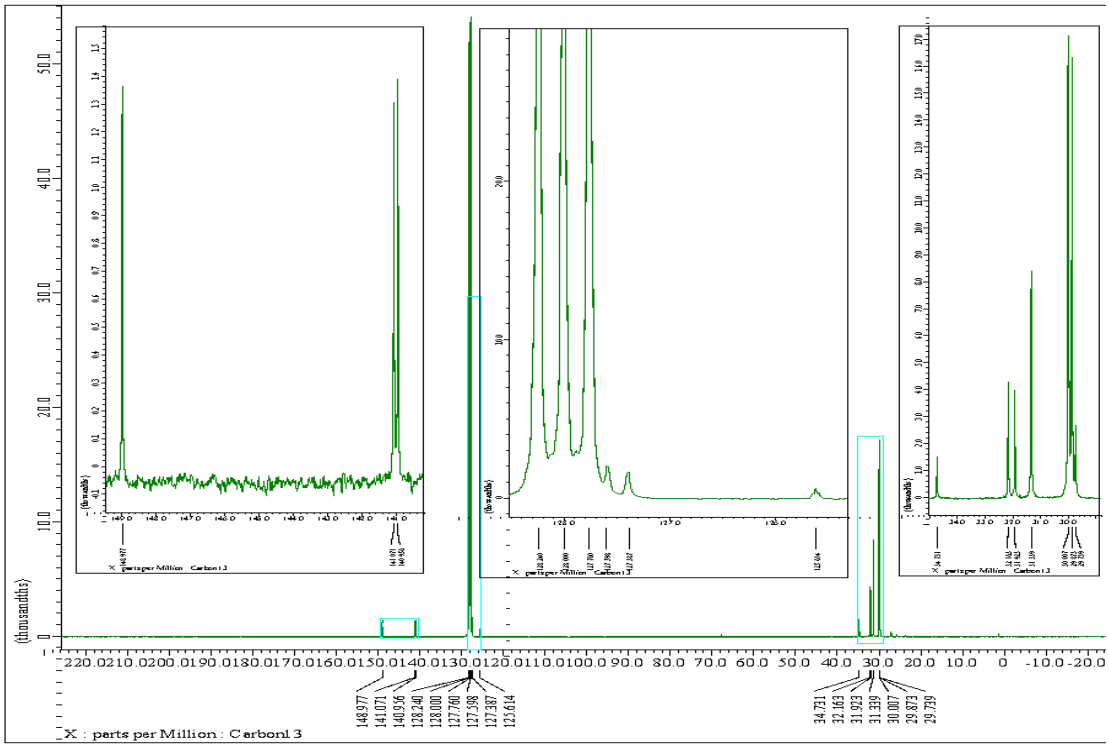

$^{t\text{Bu}}$PCP–Br, $^{31}P\{^{1}H\}$ NMR ($C_6D_6$, 162 MHz)

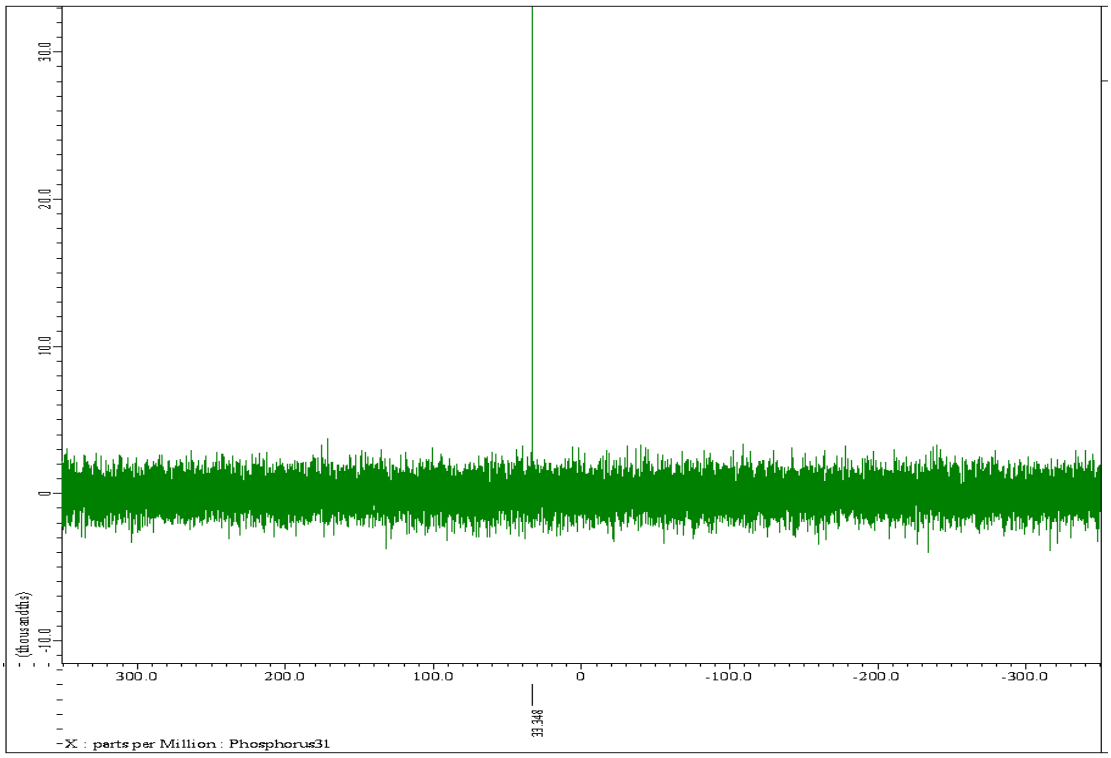

$^{ArF}$PCP–Br, $^{1}$H NMR ($C_6D_6$, 400 MHz)

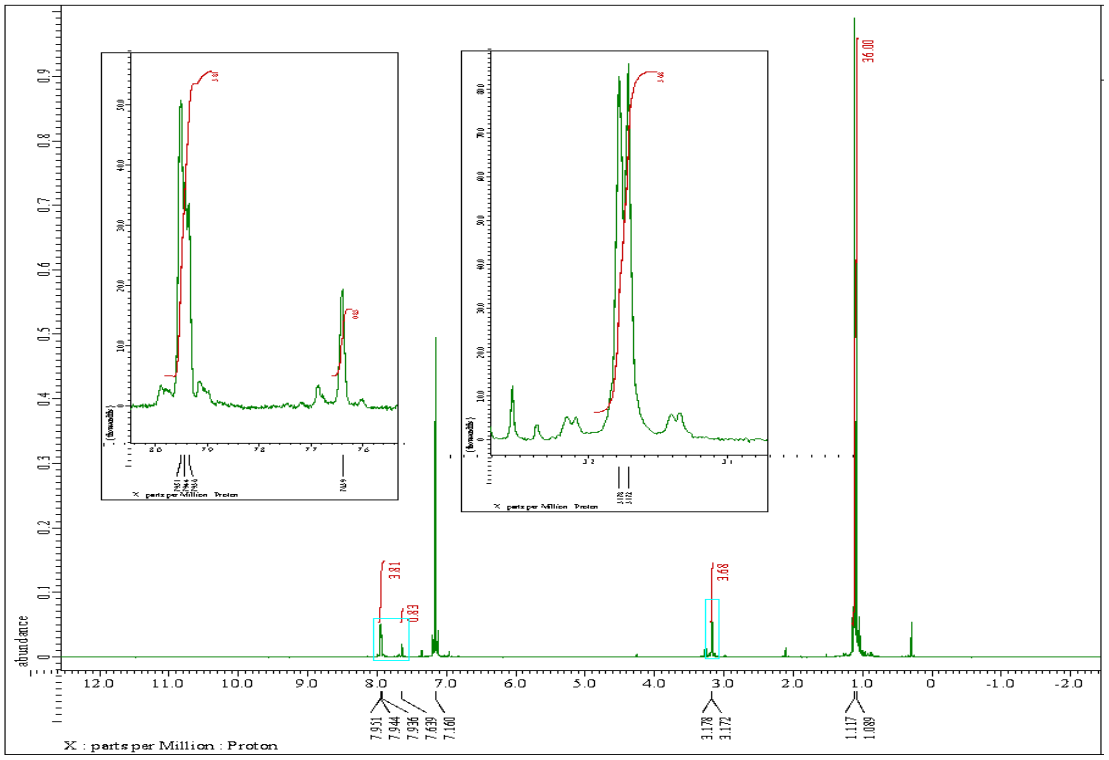


$^{ArF}$PCP–Br, $^{13}$C{$^{1}$H} NMR ($C_6D_6$, 100 MHz)

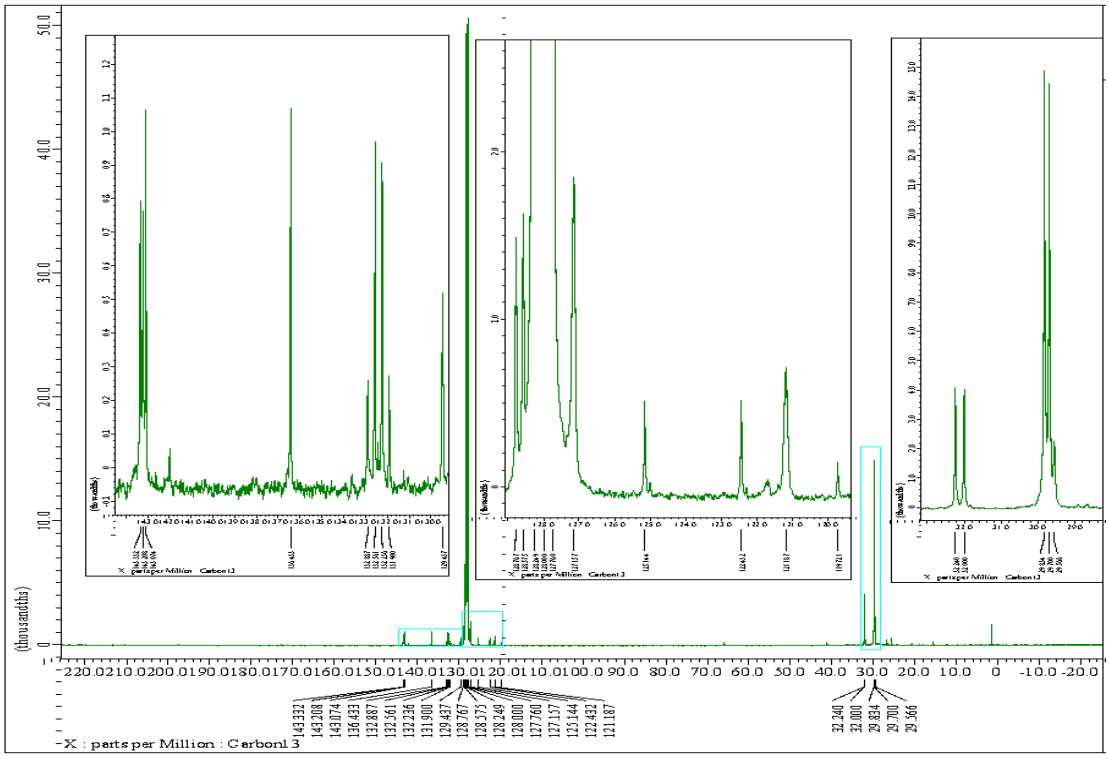

$^{ArF}$PCP–Br, $^{31}P\{^{1}H\}$ NMR ($C_6D_6$, 162 MHz)

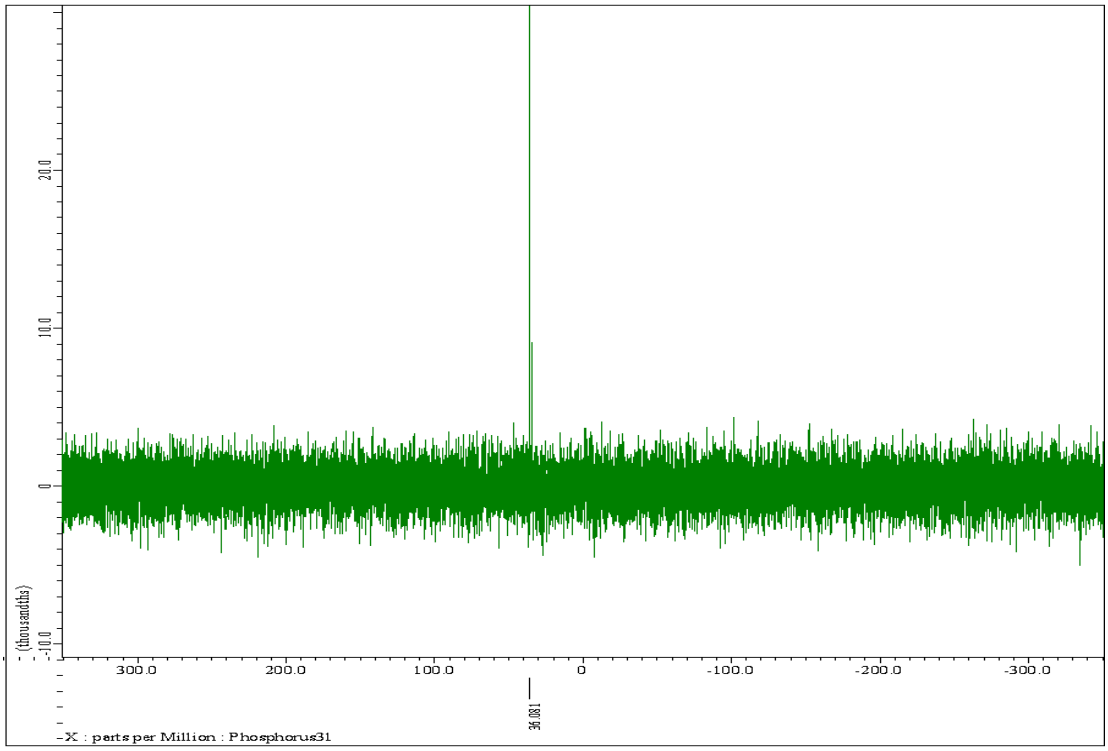


$^{ArF}$PCP–Br, $^{19}F$ NMR ($C_6D_6$, 376 MHz)

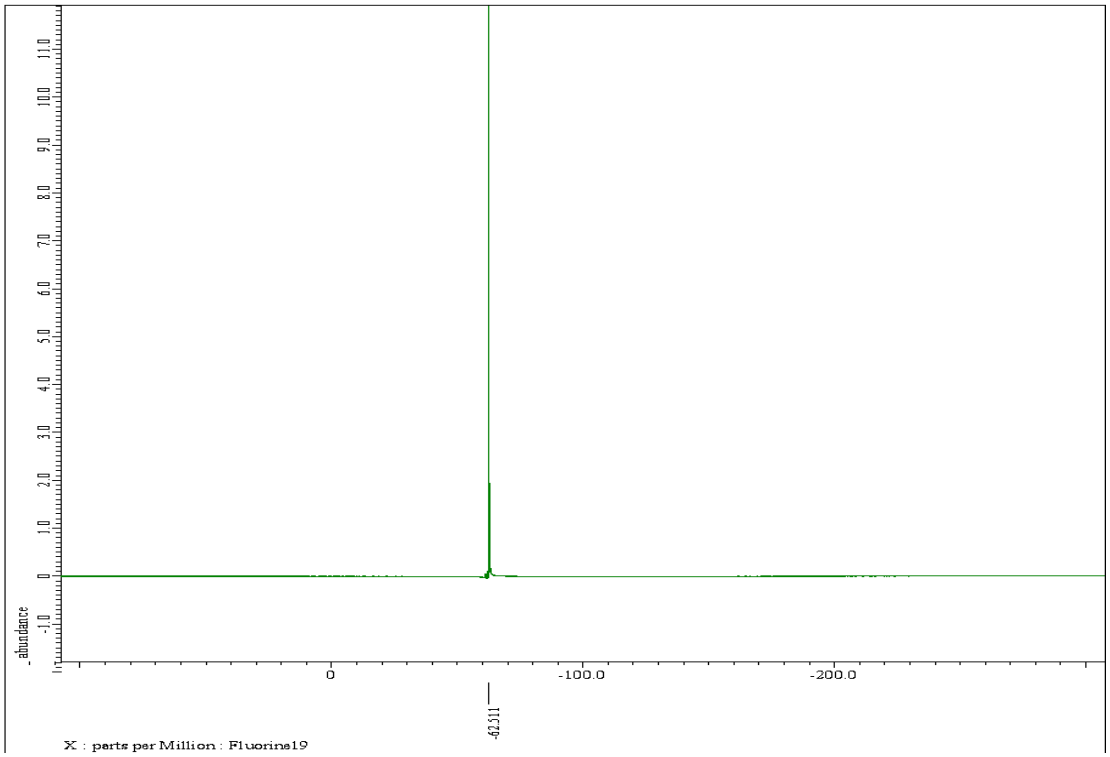

**3a**, IR (KBr)

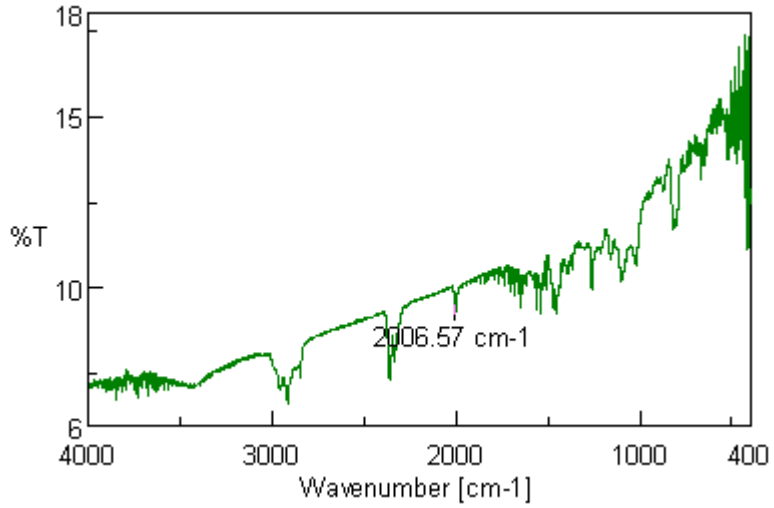


**3a**, IR (THF)

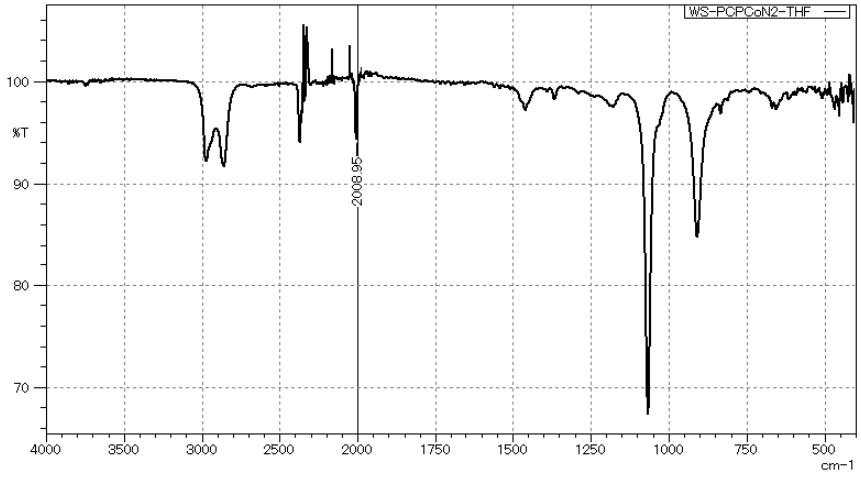


**3a**, IR (ATR)

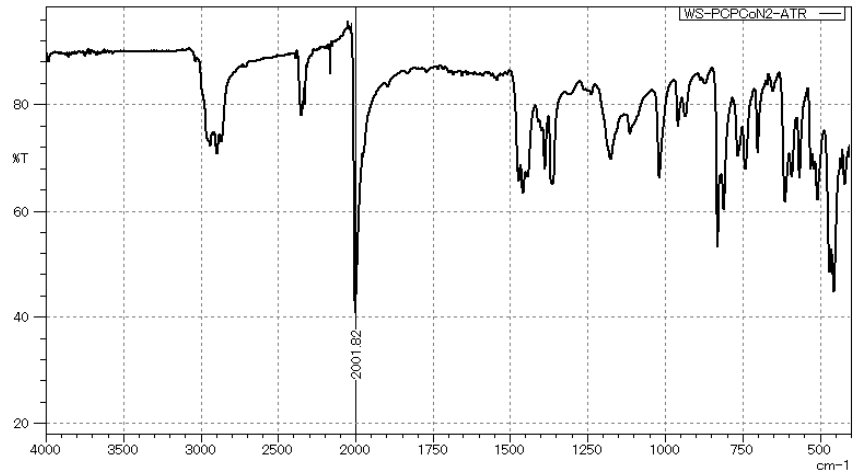


Reduction of **3a** with 10 equiv of K, IR (KBr)

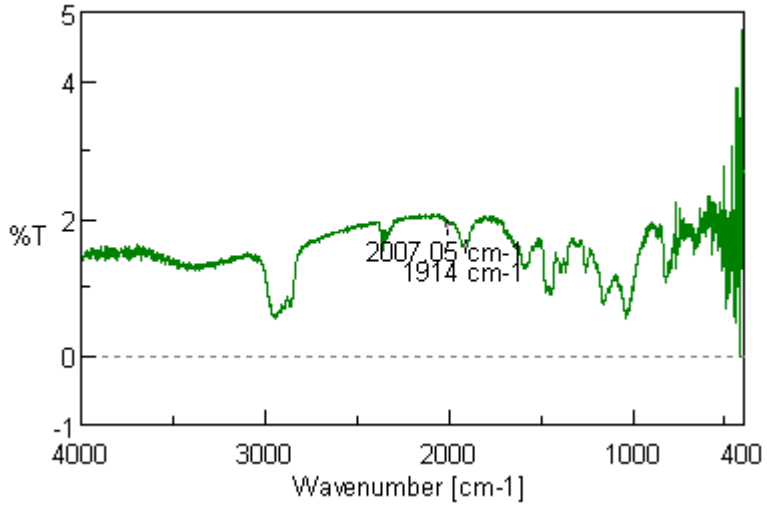
5
4
2
0
-1
%T
2007.05 cm-1
1914 cm-1
4000
3000
2000
1000
400
Wavenumber [cm-1]

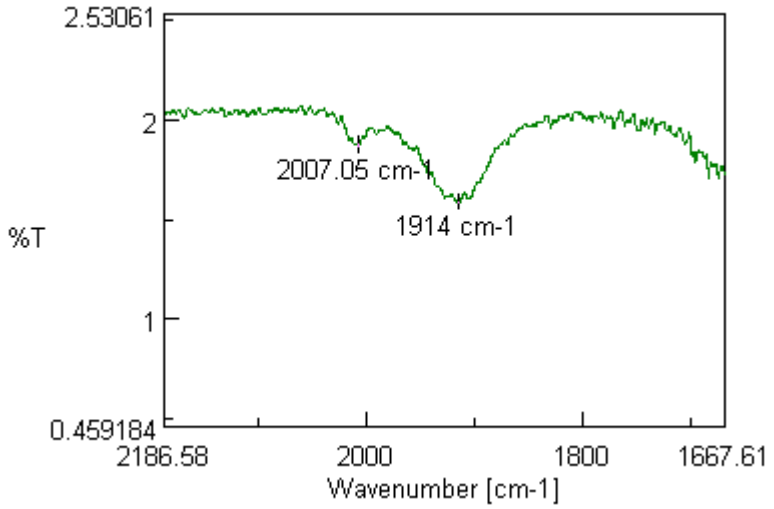
2.53061
2
1
0.459184
%T
2007.05 cm-1
1914 cm-1
2186.58
2000
1800
1667.61
Wavenumber [cm-1]

**3b**, IR (KBr)

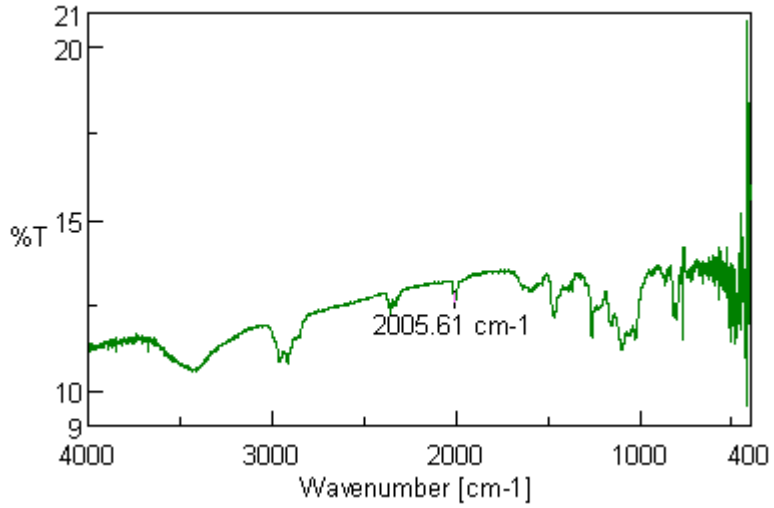


**3b**, IR (THF)

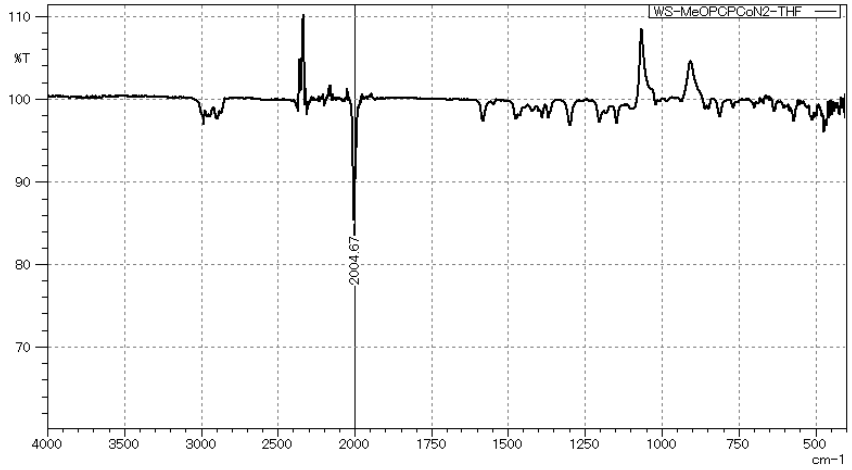


**3b**, IR (ATR)

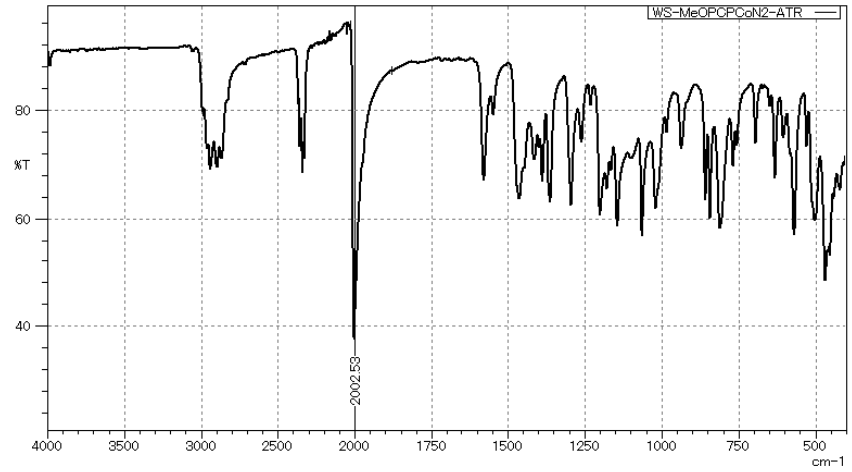

**3c**, IR (KBr)

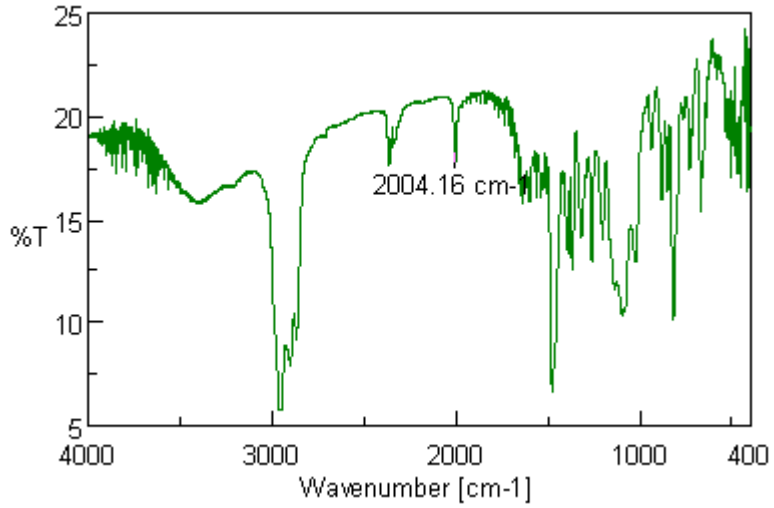


**3c**, IR (THF)

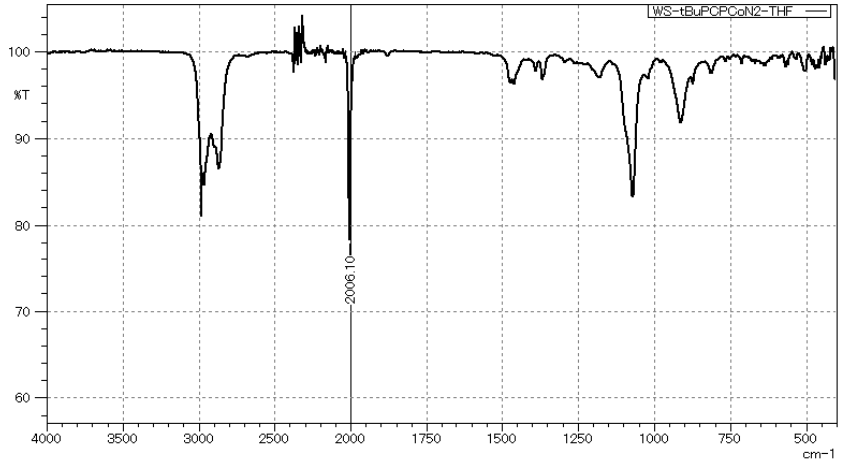


**3c**, IR (ATR)

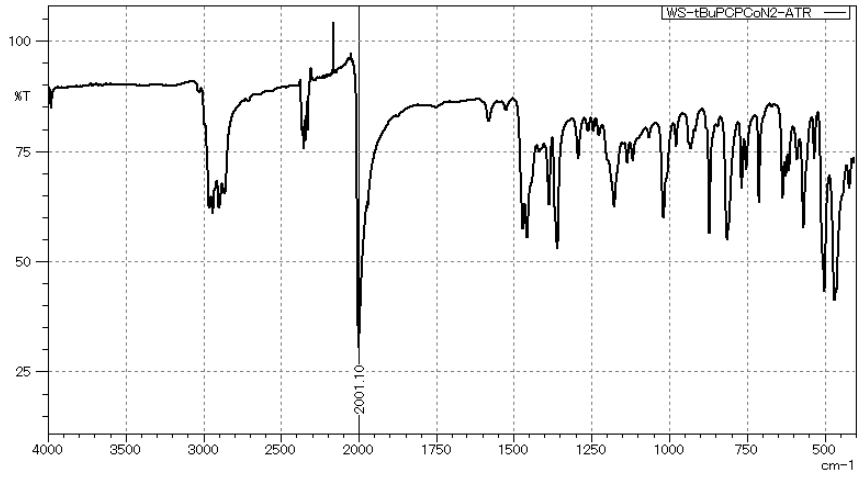

**3d**, IR (KBr)

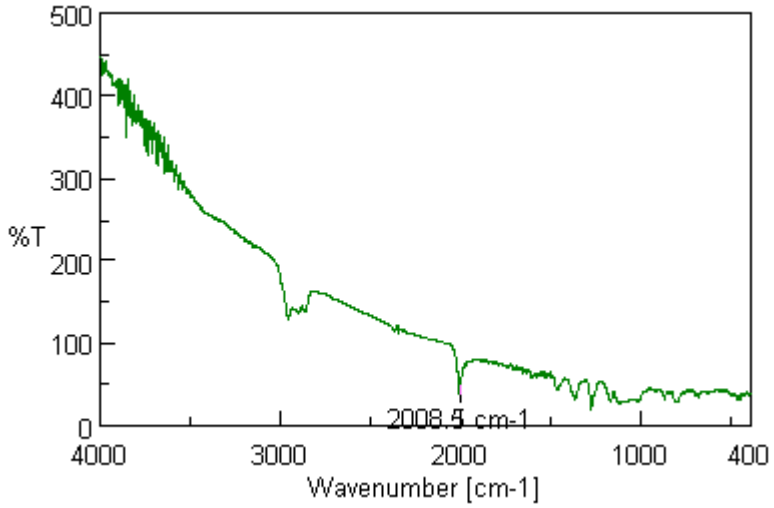


**3d**, IR (THF)

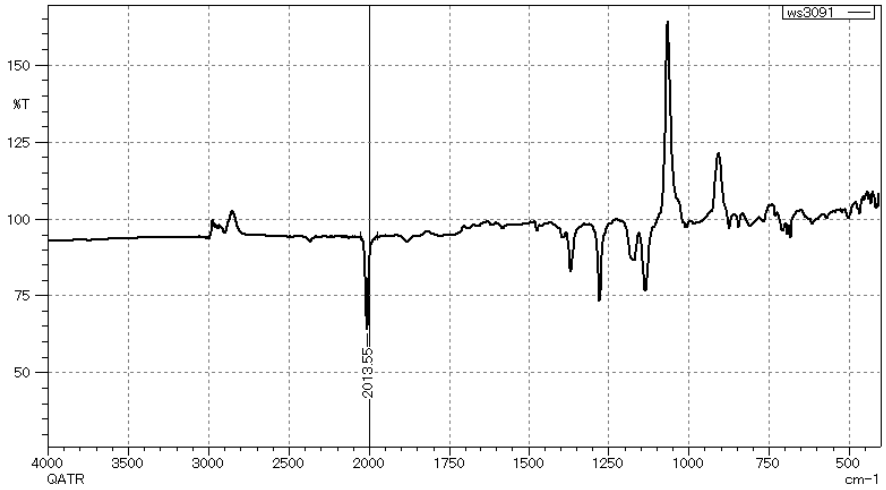


**3d**, IR (ATR)

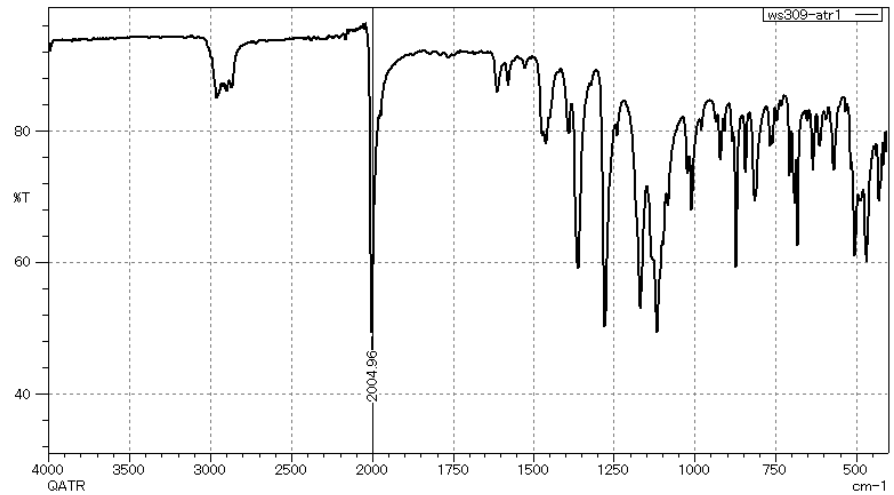

**References.**

S1 (a) Evans, D. F. *J. Chem. Soc.* **1959**, 2003. (b) Live, D. H.; Chan, S. I. *Anal. Chem.* **1970**, *42*, 791. (c) Bain, G. A.; Berry, J. F. *J. Chem. Educ.* **2008**, *85*, 532.

S2 Fan, H. Sun, H.; Peng, X. *Chem. Eur. J.* **2018**, *24*, 7671.

S3 Tashiro, M.; Yamato, T. *J. Org. Chem.* **1985**, *50*, 2939.

S4 Zhang, Z.; Edkins, R. M.; Nitsch, J.; Fucke, K.; Eichhorn, A.; Steffen, A.; Wang, Y., Marder, T. B. *Chem. Eur. J.* **2015**, *21*, 177.

S5 Meiners, J.; Friedrich, A.; Herdtweck, E.; Schneider, S. *Organometallics* **2009**, 28, *21*, 6331.

S6 Weitz, I. S.; Rabinovitz, M. *J. Chem. Soc., Perkin Trans.* **1993**, 117.

S7 Weatherburn, M. W. *Anal. Chem.* **1967**, *39*, 971.

S8 *CrysAlisPro: Data Collection and Processing Software*, Rigaku Corporation: Tokyo, Japan, 2015.

S9 *CrystalStructure 4.3: Crystal Structure Analysis Package*; Rigaku Corporation: Tokyo, Japan, 2000-2018.

S10 Sheldrick, G. M. *Acta Crystallogr., Sect. A: Found. Crystallogr.* **2008**, *A64*, 112.

S11 Sheldrick, G. M. *Acta Crystallogr., Sect. A: Found. Adv.* **2014**, *C1437*, 70.

S12 Sheldrick, G. M. *Acta Crystallogr., Sect. C: Struct. Chem.* **2015**, *C71*, 3.

S13 Spek, A. L. *Acta Crystallogr., Sect. D: Biol. Crystallogr.* **2015**, *C71*, 9.

S14 *Gaussian 09, Revision E.01*: M. J. Frisch, G. W. Trucks, H. B. Schlegel, G. E. Scuseria, M. A. Robb, J. R. Cheeseman, G. Scalmani, V. Barone, B. Mennucci, G. A. Petersson, H. Nakatsuji, M. Caricato, X. Li, H. P. Hratchian, A. F. Izmaylov, J. Bloino, G. Zheng, J. L. Sonnenberg, M. Hada, M. Ehara, K. Toyota, R. Fukuda, J. Hasegawa, M. Ishida, T. Nakajima, Y. Honda, O. Kitao, H. Nakai, T. Vreven, J. A. Montgomery, Jr., J. E. Peralta, F. Ogliaro, M. Bearpark, J. J. Heyd, E. Brothers, K. N. Kudin, V. N. Staroverov, T. Keith, R. Kobayashi, J. Normand, K. Raghavachari, A. Rendell, J. C. Burant, S. S. Iyengar, J. Tomasi, M. Cossi, N. Rega, J. M. Millam, M. Klene, J. E. Knox, J. B. Cross, V. Bakken, C. Adamo, J. Jaramillo, R. Gomperts, R. E. Stratmann, O. Yazyev, A. J. Austin, R. Cammi, C. Pomelli, J. W. Ochterski, R. L. Martin, K. Morokuma, V. G. Zakrzewski, G. A. Voth, P. Salvador, J. J. Dannenberg, S. Dapprich, A. D. Daniels, O. Farkas, J. B. Foresman, J. V. Ortiz, J. Cioslowski, and D. J. Fox, Gaussian, Inc.: Wallingford CT, 2013.

S15 Becke, A. D. *Phys. Rev*. *A* **1988**, *38*, 3098.

S16 Becke, A. D. *J. Chem. Phys.* **1993**, *98*, 5648.

S17 Lee, C.; Yang, W.; Parr, R. G. *Phys. Rev. B* **1988**, *37*, 785.

S18 Vosko, S. H.; Wilk, L.; Nusair, M. J. *Can. J. Phys.* **1980**, *58*, 1200.

S19 Grimme, S.; Antony, J.; Ehrlich, S.; Krieg, H. *J. Phys. Chem.* **2010**, *132*, 154104.

S20 Dolg, M.; Wedig, U.; Stoll, H.; Preuß, H. *J. Chem. Phys*. **1987**, *86*, 866.

S21 Andrae, D.; Häußermann, U.; Dolg, M.; Stoll, H.; Preuß, H. *Theor. Chim. Acta.* **1990**, *77*, 123.

S22 Ditchfield, R.; Hehre, W. J.; Pople, J. A. *J. Chem. Phys*. **1971**, *54*, 724.

S23 Hehre, W. J.; Ditchfield, R.; Pople, J. A. *J. Chem. Phys.* **1972**, *56*, 2257.

S24 Hariharan, P. C.; Pople, J. A. *Theor. Chem. Acc.* **1973**, *28*, 213.

S25 Francl, M. M.; Pietro, W. J.; Hehre, W. J.; Binkley, J. S.; Gordon, M. S.; DeFrees, D. J.; Pople, J. A. *J. Chem. Phys*. **1982**, *77*, 3654.

S26 Tomasi, J.; Mennucci, B.; Cammi, R. *Chem. Rev*. **2005**, *105*, 2999.

S27 Weigend, F.; Ahlrichs, R. *Phys. Chem. Chem. Phys*. **2005**, *7*, 3297.

S28 Weigend, F. *Phys. Chem. Chem. Phys.* **2006**, *8*, 1057.